

Discriminating fluvial fans and deltas: Channel network morphometrics reflect distinct formative processes

Luke Gezovich^{1*}, Piret Plink-Björklund¹, Jack Henry^{1,2}

¹ Colorado School of Mines, Geology & Geologic Engineering, 1500 Illinois Street, Golden, CO, 80401

² Rice University, Earth, Environmental and Planetary Sciences, 6100 Main St., Houston, TX, 77005-1827

Correspondence to: Luke Gezovich (lukegezovich@mines.edu)

Abstract

Recent recognition of a new type of fluvial system – fluvial fans – introduces a fan-shaped channel network that appears similar to that of river-dominated deltas. Deltas form where rivers enter lakes and oceans, while fluvial fans are terrestrial landforms. However, fluvial fans can reach the shorelines of oceans or lakes, and in such cases the distinction between fluvial fan and river-dominated delta channel networks becomes ambiguous. We currently lack fundamental understanding of these two landforms’ morphometric differences, despite their high socioeconomic significance, vulnerability to natural hazards, and key differences in how these landforms respond to global climate change and urbanization. Here we review the relevant conceptual differences in delta and fluvial fan network morphodynamics, propose a set of quantitative morphometric criteria to distinguish fluvial fan and delta channel networks, and test these criteria on 40 deltas and 40 fluvial fans from across the world. This initial attempt to contrast and distinguish deltas and fluvial fans based on their channel network morphometrics demonstrates that quantifying channel network angles (mean of 74.0° for deltas and 55.0° for fluvial fans) and trends in normalized channel widths and lengths provide efficient criteria, but some ambiguities remain that need to be resolved in future work. This research advances our mechanistic understanding of fluvial fan and delta channel networks and the recognition of modern and ancient landforms on Earth and other planetary bodies, such as Mars and Saturn’s moon Titan.

Plain Language Summary

Fluvial fans are a newly recognized type of river system that look like river deltas, especially when they reach lakes or oceans. This study explores how to tell them apart by measuring the size and layout of channels in these fan-shaped landforms. Understanding these differences helps to predict how these landforms respond to climate change and urbanization, and to identify them on Mars and other planetary bodies.

36 1. Introduction

37 River deltas are depositional landforms that form where rivers enter lakes or oceans. They are
38 home to over half a billion people, host abundant and biodiverse ecosystems, and function as both
39 economic and agricultural hubs (Saito et al., 2007; Tejedor et al., 2015). Deltas are global change hotspots
40 highly vulnerable to urbanization and climate change, which can aggravate coastal hazards and cause sea-
41 level rise (Giosan et al., 2014; Syvitski et al., 2009), and reduce sediment supply due to river damming
42 and artificial levees causing the drowning of deltas (Blum and Roberts, 2009; Giosan et al., 2014;
43 Nienhuis et al., 2020; Paola et al., 2011; Syvitski et al., 2009). The form and function of deltas is
44 intimately linked to the evolving structure of their channel networks that determine how deltas distribute
45 sediment and nutrients (Passalacqua, 2017; Pearson et al., 2020; Tejedor et al., 2017). Delta channel
46 network morphology results from an intricate balance between sediment erosion and deposition from
47 river, tide, and wave energy fluxes. River fluxes create distributary channels and islands, tides roughen
48 the shoreline and widen the channels, and waves smooth the shoreline and decrease the number of
49 distributary channels (Broaddus et al., 2022; Galloway, 1975; Nienhuis et al., 2015, 2018; Paniagua-
50 Arroyave and Nienhuis, 2024; Vulis et al., 2023). Deltas dominated by river energy fluxes (river-
51 dominated deltas) (Broaddus et al., 2022; Galloway, 1975; Nienhuis et al., 2015, 2018; Paniagua-
52 Arroyave and Nienhuis, 2024; Vulis et al., 2023) characteristically form fan-shaped landforms with
53 complex distributary channel networks (Fig. 1). In these deltas, channel network topology is defined by
54 mouth bar deposition and consequent distributary channel bifurcation (Bates, 1953; Edmonds and
55 Slingerland, 2007; Wright, 1977).

56 Fluvial fans are another type of fan-shaped landform with channel networks that share
57 morphological similarities with the river-dominated delta channel networks (Fig. 2). Fluvial fans are a
58 relatively newly acknowledged type of fluvial landform (Ventra and Clarke, 2018; Weissmann et al.,
59 2010), which forms via river avulsions or “channel jumps” across low-gradient floodplains (Chakraborty
60 et al., 2010; Martin and Edmonds, 2023; North and Warwick, 2007). Rivers have been traditionally
61 regarded as sediment transfer or bypass zones in source-to-sink systems (Allen, 2008; Fielding et al.,
62 2012), whereas fluvial fans are net depositional and build significant stratigraphic thicknesses
63 (Chakraborty et al., 2010; Moscariello, 2018; Weissmann et al., 2015). Fluvial fans are also called “wet”
64 fluvial-dominated alluvial fans (Schumm, 1977), megafans (Singh et al., 1993), or distributive fluvial
65 systems (DFS) (Weissmann et al., 2010). Fluvial fans are distinct landforms from alluvial fans – which
66 form by a combination of gravitational and streamflow processes, feature steep gradients (typically 2–
67 12°), and have a relatively small radius typically less than 10 km (Blair and McPherson, 1994;
68 Moscariello, 2018). Fluvial fans form some of the largest terrestrial landforms on Earth (10^3 – 10^5 km² in
69 surface area) (Horton and DeCelles, 2001; Leier et al., 2005) and have low gradients (0.0018–1.5°)

70 (Hartley et al., 2010). Fluvial fans are abundant across Earth, and they form in diverse climatic and
71 tectonic settings (Hartley et al., 2010; Ventra and Clarke, 2018; Weissmann et al., 2010).

72 Like deltas, fluvial fans are home to hundreds of millions of people, and these highly dynamic
73 landforms are critical for their livelihood – supporting agriculture, fisheries, and freshwater access. They
74 also experience catastrophic floods; for example, the Kosi fluvial fan floods have led to large numbers of
75 casualties and displaced populations (Sinha, 2009; Syvitski and Brakenridge, 2013). While fluvial fans
76 are terrestrial landforms, they can reach the shorelines of oceans (Fig. 2b) or lakes (Figs. 2a, 2d, and 2i).
77 In such cases the distinction between fluvial fan and river-dominated delta channel networks becomes
78 ambiguous, while wave- and tide-dominated deltas have distinctly recognizable morphologies (Broaddus
79 et al., 2022; Galloway, 1975; Nienhuis et al., 2015, 2018; Paniagua-Arroyave and Nienhuis, 2024; Vulis
80 et al., 2023). We currently lack quantitative morphometric criteria for distinguishing river-dominated
81 delta and fluvial fan channel networks, despite their socioeconomic significance, key differences in their
82 natural hazard vulnerabilities, and in how they respond to global change.

83 Numerous fan-shaped landforms with channel networks have also been identified on other planetary
84 bodies such as Mars (Malin and Edgett, 2015; Ori et al., 2000; Wood, 2006) and Saturn’s moon Titan
85 (Radebaugh et al., 2018; Wall et al., 2010; Witek and Czechowski, 2015). Deltas on planetary bodies are
86 important indicators of paleo-shorelines and have been utilized to reconstruct the shorelines and water
87 levels of ancient lakes and oceans on Mars (Di Achille and Hynek, 2010). However, Martian paleo-ocean
88 shoreline reconstructions have so far yielded mixed results (De Toffoli et al., 2021). This discrepancy
89 could perhaps arise because shoreline-bound deltas have not been effectively distinguished from fluvial
90 fans on Mars, which may form thousands of kilometers inland from shorelines (Bramble et al., 2019;
91 Limaye et al., 2023; Tebolt and Goudge, 2022). Deltas also offer attractive targets for mission sites in
92 search of life due to their habitability and high biosignature preservation potential, as exemplified by the
93 selection of Jezero Crater for NASA’s *Perseverance* rover, *Ingenuity* helicopter, and future Mars Sample
94 Return mission (Farley et al., 2020). Distinguishing deltaic and fluvial fan paleo-channel networks on
95 other planetary bodies is even more ambiguous, especially if the lakes and oceans are no longer present.

96 Over time, the accumulation of biogenic and sedimentary materials distributed via channel networks
97 contributes to the construction of stratigraphy. Fluvial fans and deltas are both net depositional systems
98 characterized by spatially diminishing water surface slopes that reduce sediment transport capacity,
99 thereby producing spatiotemporal convergence and deposition of sediment (Ganti et al., 2014).
100 Consequently, in addition to their socioeconomic significance, both landforms significantly contribute to
101 the stratigraphic record, and their deposits can be used to decipher past environmental conditions. High
102 deposition rates in fluvial fans and deltas promote the preservation of environmental change signals in the
103 sedimentary record (Trampush and Hajek, 2017). Similar to modern river-dominated deltas and fluvial

104 fans, we lack morphometric criteria to distinguish these two fan-shaped channel networks in the
105 sedimentary record, such as in seismic datasets.

106 This study is motivated by developing quantitative morphometric distinction criteria for fluvial fan
107 and river-dominated delta channel networks. Prior work has established quantitative morphological
108 criteria for describing deltaic channel networks and linked these characteristics to theory (Chen et al.,
109 2021; Coffey and Shaw, 2017; Edmonds et al., 2011; Edmonds and Slingerland, 2007; Fagherazzi et al.,
110 2015; Ke et al., 2019; Passalacqua, 2017; Pearson et al., 2020; Tejedor et al., 2015, 2017). However, there
111 are no existing quantitative criteria to characterize fluvial fan channel networks or to differentiate the two
112 landforms. To develop such criteria, we review the relevant conceptual differences in delta and fluvial fan
113 network morphodynamics, propose quantitative morphometric criteria to distinguish fluvial fan and delta
114 channel networks, and test these criteria on 40 deltas and 40 fluvial fans (Supplementary Data) from
115 across the globe (Fig. 3). We test the robustness of the approach by analyzing differences in channel
116 network morphometrics concerning the size and gradient of the systems, lake versus ocean terminations
117 and tide versus wave influences in deltas, and fan termination styles in fluvial fans. We assess how
118 effectively the proposed methods distinguish fluvial fans from river-dominated deltas and examine why
119 this distinction matters under global change. This work serves to improve our mechanistic understanding
120 of fluvial fan and delta evolution, and their accurate recognition on Earth, other planetary bodies, and in
121 the sedimentary record.

122 **2. Delta and Fluvial Fan Channel Network Morphodynamics**

123 The nature of channel networks is dependent on distinct morphodynamic processes responsible for
124 their formation (Edmonds and Slingerland, 2007; Fagherazzi et al., 2015; Tejedor et al., 2015). Below we
125 analyze differences in delta and fluvial fan morphodynamics and review existing morphometric criteria
126 for quantifying deltaic distributary channel networks. Our review is not comprehensive; rather, it focuses
127 on the specific processes that govern the formation of the morphometric characteristics that we can then
128 use for distinction of these two landforms, namely channel network angles, and downstream changes in
129 channel widths and lengths. There are other important characteristics of deltaic channel networks, linked
130 to water and sediment discharge distribution, entropy, and connectivity (Chen et al., 2021; Ke et al., 2019;
131 Passalacqua, 2017; Pearson et al., 2020; Tejedor et al., 2015, 2017). These aspects are not considered in
132 this review, because they are outside the scope of this study that seeks to distinguish deltaic and fluvial
133 fan channel networks using easily applicable morphometric criteria that can be used for both deltaic and
134 fluvial fan networks.

135
136
137

138 2.1 River Deltas

139 Deltas (Fig. 1) form only where a river enters a standing body of water. Here, the transport capacity
140 of the turbulent jet decreases, and the “parent” stream jet flow experiences both lateral and bed friction,
141 causing the flow to decelerate and rapidly expand laterally (Bates, 1953; Edmonds and Slingerland, 2007;
142 Jerolmack and Swenson, 2007; Wright, 1977). As a result, the transport capacity of the turbulent jet
143 decreases and sediment is deposited as a mouth bar basinward of the river mouth (Edmonds and
144 Slingerland, 2007). The process of mouth bar deposition and growth eventually leads to the downstream
145 branching, or *bifurcation*, of a single (parent) channel into two daughter channels (Axelsson, 1967;
146 Coffey and Shaw, 2017; Edmonds and Slingerland, 2007) (Fig. 4a). These daughter channels are
147 separated by an island or shallow bay where sediment transport is significantly reduced or nonexistent,
148 and flow is unchannelized (Coffey and Shaw, 2017). Mouth bar deposition and resultant channel
149 bifurcation repeat multiple times, leading to the seaward advancement of the shoreline and the
150 construction of a delta distributary channel network (Edmonds and Slingerland, 2007; Olariu and
151 Bhattacharya, 2006) (Fig. 4a).

152 Deltas also experience channel avulsions or “channel jumps” at the lobe-level (Slingerland and Smith,
153 2004). These deltaic avulsions occur within a region of high-water surface slope variability caused by
154 backwater hydrodynamics that are characterized by spatial flow deceleration and deposition during low
155 flows, and flow acceleration and bed scour with high flows (Brooke et al., 2022; Chatanantavet et al.,
156 2012; Chatanantavet and Lamb, 2014). As the backwater zone sets the location for avulsion in deltas
157 (Chatanantavet et al., 2012), they are strongly controlled by hydrodynamics in their receiving basin, like
158 mouth-bar-driven bifurcations. As a result, the delta lobe size is generally consistent and the lobe avulsion
159 node migrates downstream commensurate with shoreline progradation (Ganti et al., 2014), as influenced
160 by flood frequency, sediment supply, or sea-level rise (Brooke et al., 2022). These avulsions episodically
161 rearrange the depocenter at the delta lobe scale, whereas the substantially more frequent mouth-bar-driven
162 bifurcations generate the topology of the delta distributary channel networks (Bentley et al., 2016;
163 Edmonds and Slingerland, 2007).

164 Resultant delta channel networks have a specific angle at which distributary channels bifurcate (Fig.
165 4b) (Coffey and Shaw, 2017), because a mouth-bar-driven bifurcation will grow toward an equilibrium
166 angle of 72° to maximize flux at the two channel tips (Coffey and Shaw, 2017; Devauchelle et al., 2012;
167 Ke et al., 2019; Mahon et al., 2024). First described in tributary networks, this theoretical angle arises
168 from diffusive groundwater flow (Devauchelle et al., 2012). Testing of this concept reports mouth-bar-
169 driven bifurcation angles of $70.4^\circ \pm 2.6^\circ$ ($n = 9$) in natural deltas (Coffey and Shaw, 2017), and $68.3^\circ \pm$
170 8.7° ($n = 21$) (Coffey and Shaw, 2017) and $74.1^\circ \pm 7.7^\circ$ ($n = 13$) (Federici and Paola, 2003) in
171 experimental deltas.

172 Deltaic channel networks tend to consistently self-organize (Edmonds et al., 2011; Fagherazzi, 2008)
173 and exhibit a theoretical fractal pattern of decreasing channel widths and lengths associated with
174 increasing bifurcation order (Edmonds et al., 2011; Edmonds and Slingerland, 2007; Hariharan et al.,
175 2022; Seybold et al., 2017; Wolinsky et al., 2010) (Fig. 4a). Edmonds and Slingerland (2007) show that
176 channel width trends align with hydraulic geometric scaling: as the discharge of a parent channel divides
177 into the discharge for two resultant daughter channels, the daughter channel dimensions decrease as they
178 scale with bankfull discharge. Channel lengths decrease downstream with each successive bifurcation
179 because the jet momentum flux and consequent average grain transport distance decrease downstream,
180 causing new mouth bar deposition and accompanying bifurcations to occur closer to the previous
181 bifurcation node for a given channel (Edmonds and Slingerland, 2007) (Figs. 4a, 4b).

182 The nature of delta channel networks is further affected by waves and tides (Broaddus et al., 2022;
183 Geleynse et al., 2011; Jerolmack and Swenson, 2007) where the relative strength of river, wave, and tide
184 processes determines whether deltas are river, wave, or tide dominated (Galloway, 1975; Nienhuis et al.,
185 2015, 2018; Paniagua-Arroyave and Nienhuis, 2024; Vulis et al., 2023). Since wave- and tide-*dominated*
186 deltas exhibit distinct morphologies from river-dominated delta and fluvial fan channel networks, they are
187 not considered in this study (see Methods for more information on classification).

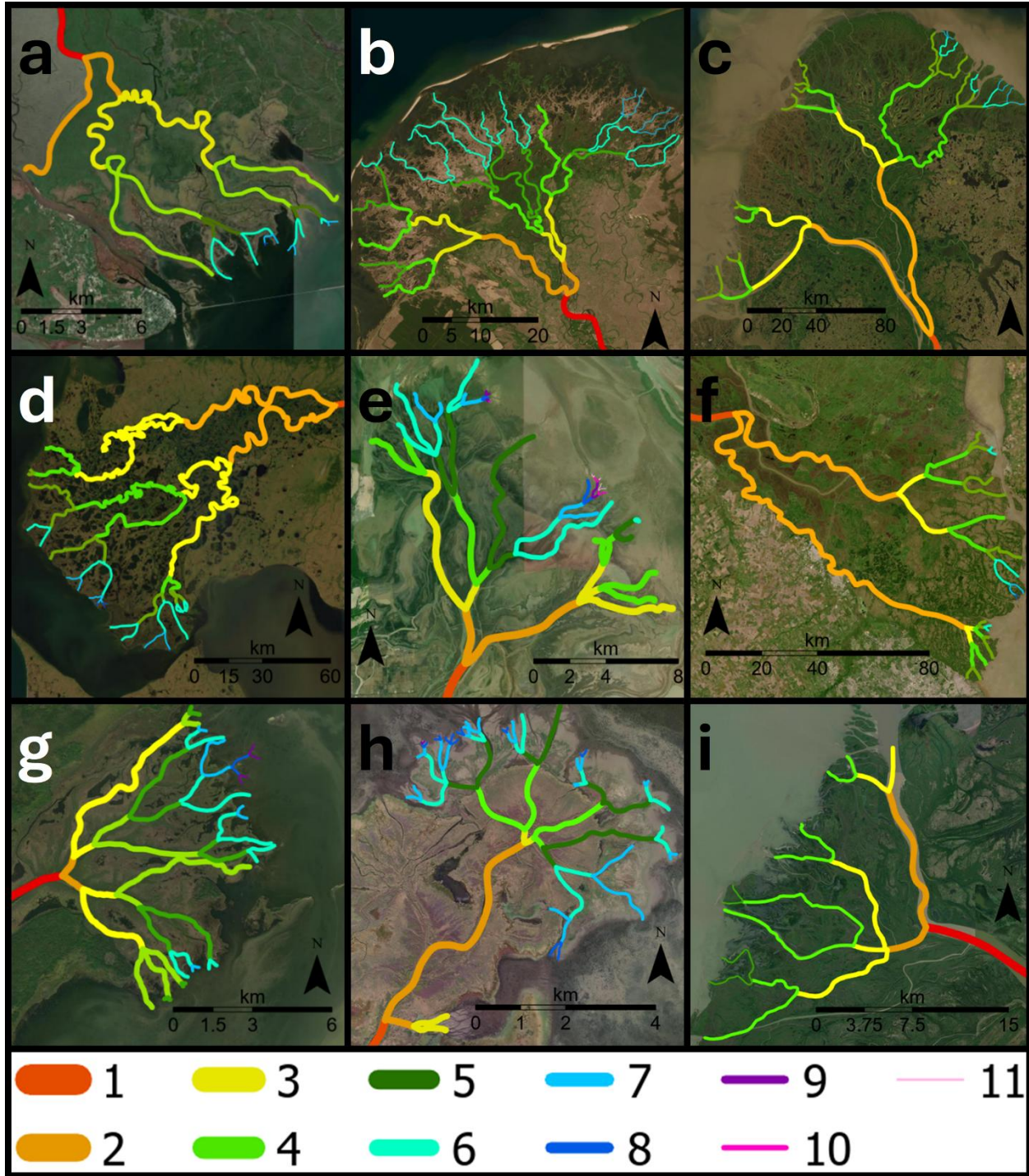


Figure 1: Examples of delta channel networks: (a) Apalachicola, (b) Selenga, (c) Yukon, (d) Kobuk, (e) Poyang Lake, (f) Parana (g) Saskatchewan, (h) Mamawi lake, (i) Slave deltas. The colors indicate channel hierarchy (see Methods). Base imagery from Esri's World Imagery basemap (© Esri, DigitalGlobe, GeoEye, i-cubed, USDA FSA, USGS, AEX, Getmapping, Aerogrid, IGN, IGP, swisstopo, and the GIS User Community). Colors and relative line thicknesses indicate channel hierarchy (see Methods), with the widest lines representing order 1 channels and progressively thinner lines representing higher channel orders.

189 2.2 Fluvial Fans

190 Fluvial fans are fan-shaped landforms that form by river avulsions or “channel jumps” across a low-
191 gradient floodplain (Chakraborty et al., 2010; Martin and Edmonds, 2023). In contrast to deltas where
192 mouth-bar-driven bifurcations and backwater-driven avulsions are strongly controlled by hydrodynamics
193 near a receiving basin of standing water (Brooke et al., 2022; Chatanantavet et al., 2012; Ganti et al.,
194 2014), *avulsions* that form fluvial fans are driven by a topographic slope break (Ganti et al., 2014; Martin
195 and Edmonds, 2023). Increased likelihood of avulsions at the fan apex is a consequence of the gradient
196 reduction that triggers in-channel sediment aggradation (Parker et al., 1998). These avulsions result from
197 high channel bed aggradation rates that are considerably higher than on the surrounding floodplains
198 (Pizzuto, 1987). Set up by in-channel aggradation, avulsions develop where a channel changes its course
199 due to channel superelevation (Bryant et al., 1995; Gearon et al., 2024; Mohrig et al., 2000) or a more
200 favorable (steeper) gradient at channel flanks (Gearon et al., 2024; Jones and Schumm, 1999; Slingerland
201 and Smith, 2004). Since the slope break controls the location of the fluvial fan’s apex, this avulsion node
202 is topographically pinned at this change in gradient, unlike in deltas (Ganti et al., 2014; Brooke et al.,
203 2022). Partial or full avulsions also occur further downfan, involving local gradient or discharge
204 decreases, or crevassing processes (Assine, 2005; Chakraborty et al., 2010; Donselaar et al., 2013; Gearon
205 et al., 2024) (Fig. 2).

206 Fluvial fan channel networks thus result through repeated nodal style avulsions (Slingerland and
207 Smith, 2004) that typically shift the primary river to different regions of the fan (Chakraborty et al., 2010;
208 Martin and Edmonds, 2023; North and Warwick, 2007). These avulsions superimpose new channel
209 positions on paleo-channel locations and can split channels by partial avulsions and crevasses. This
210 generates channel and paleo-channel branching formed by processes distinct from deltas (North and
211 Warwick, 2007) (Figs. 4c, 4d), where channel branching is predominantly caused by mouth-bar-driven
212 bifurcations. In fluvial fans, channel branching is related to avulsions, which generate channel networks
213 that are predominantly paleo-channel networks rather than active channel networks like in deltas
214 (Chakraborty et al., 2010; North and Warwick, 2007). Multiple channels can actively transmit discharge
215 at partial avulsions, such as during major river floods.

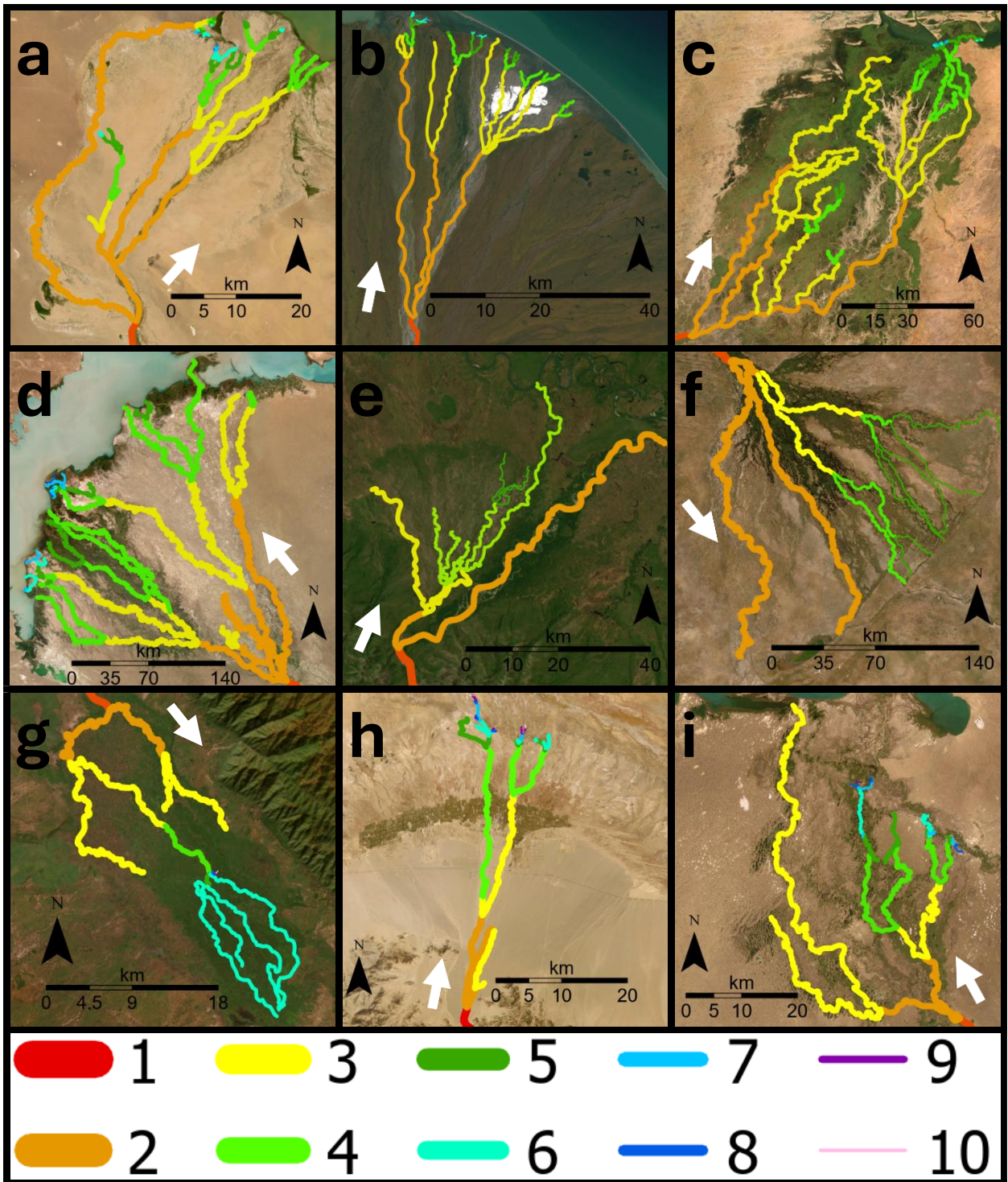
216 Downfan decreases in channel width have been well documented in modern and ancient fluvial fans
217 (Davidson et al., 2013; Kelly and Olsen, 1993; Nichols, 1987; Nichols and Fisher, 2007; Owen et al.,
218 2015; Wang and Plink-Björklund, 2019; Weissmann et al., 2010), linked to discharge losses to floodplain
219 processes, infiltration into the loose sediments of the fan, and evapotranspiration (Davidson et al., 2013;
220 Hartley et al., 2010; Horton and DeCelles, 2001; Weissmann et al., 2010). However, some fluvial fan
221 channels have also been shown to widen downstream, possibly due to changes in channel planform or
222 aspect ratio, discharge contribution from groundwater, or discharge capture from adjacent rivers

223 (Chakraborty et al., 2010; Davidson et al., 2013). Fluvial fan channel networks have been studied for
224 qualitative descriptions of channel planform morphology (Davidson et al., 2013; Hartley et al., 2010;
225 Weissmann et al., 2010) and scaling relationships (Davidson et al., 2013; Davidson and Hartley, 2014).
226 Modeling establishes a relationship between the fluvial fan shape and avulsion dynamics, like avulsion
227 trigger period and abandoned channel dynamics (Edmonds et al., 2022; Martin and Edmonds, 2023).

228 Fluvial fans are distinct landforms from alluvial fans that feature steep gradients (typically 2–12°),
229 have a relatively small radial distance typically less than 10 kilometers, and lack channel networks (Blair
230 and McPherson, 1994; Moscariello, 2018). Although surface channels may occur on alluvial fans, these
231 are transient features formed by surface erosion, and do not construct alluvial fans, which form by a
232 combination of gravitational and sheet flood processes (Blair and McPherson, 1994; Moscariello, 2018).
233 Thus, alluvial fans are not considered here as they are distinct from fluvial fan channel networks that form
234 by river avulsions.

235 **2.3 Morphometric Criteria for Recognition of Delta and Fluvial Fan Channel Networks**

236 Based on the above differences in delta and fluvial fan morphodynamics, we hypothesize that the
237 morphometric differences in their channel networks can be quantified. Based on prior work, we expect
238 river-dominated delta channel networks to display downstream decreasing channel widths and lengths
239 with increasing bifurcation order (Edmonds and Slingerland, 2007; Seybold et al., 2007; Wolinsky et al.,
240 2010), and have an average channel network angle of approximately 72° (Coffey and Shaw, 2017). These
241 metrics should differ in fluvial fans, because the channel networks are built by river avulsions rather than
242 mouth-bar-driven bifurcations. However, delta networks also experience (lobe-scale) avulsions, and we
243 expect some overlap in the network angles. Below, we test these morphometric criteria on 40 river-
244 dominated delta and 40 fluvial fan channel networks (Fig. 3).



245
246
247
248
249
250

251 **3. Dataset and Methods**

252 Although automated channel mapping tools like ChannelExtractor in TopoToolbox (Schwanghart and
253 Kuhn, 2010) and RivaMap (Isikdogan et al., 2017) exist, these methods rely on either terrain-based flow
254 routing or the detection of active surface water, typically based on spectral characteristics, to delineate
255 river channels. However, fluvial fan channel networks are predominantly composed of paleo-channels
256 that lack both clear topographic expression and surface water signatures. Both delta and fluvial fan
257 channels can also be only a few meters wide, often falling below the spatial resolution of commonly
258 available DEMs and remote sensing imagery. In such settings, the coarse resolution and smoothing of
259 subtle terrain in DEMs, especially in low-relief environments, further limit the effectiveness of automated
260 extraction. As a result, we are constrained to manual digitization, as described below.

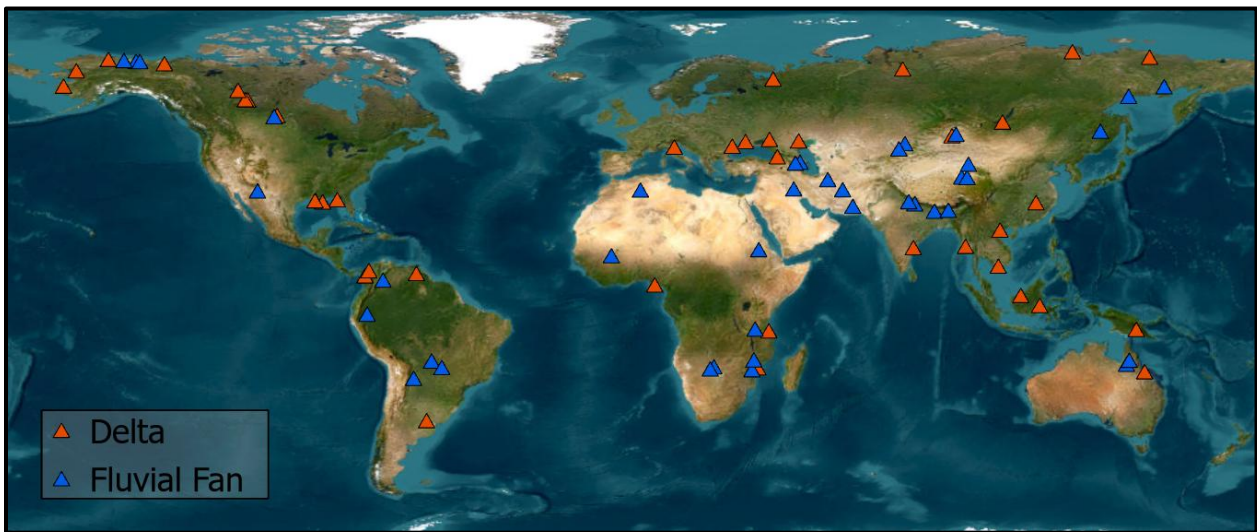


Figure 3: Map of deltas and fluvial fans in this study. Base imagery from Esri’s World Imagery basemap (© Esri, DigitalGlobe, GeoEye, i-cubed, USDA FSA, USGS, AEX, Getmapping, Aerogrid, IGN, IGP, swisstopo, and the GIS User Community).

261 **3.1 Channel Order**

262 To establish channel order in networks, we follow Dong et al. (2016). Their method follows a simple
263 rule: bifurcations produce downstream increasing channel order through channels that branch. To be
264 considered a channel of a higher order, the resultant channels must not merge downstream. When a first-
265 order channel bifurcates, two second-order channels develop downstream of this bifurcation. When these
266 two channels subsequently bifurcate, two new pairs of third-order channels form, and so on (Figs. 4a, 4b).
267 All channels from the first instance of branching up to and including those that enter a body of water or
268 terminate on land are measured. Identification of bifurcation nodes follows Edmonds et al. (2011), such
269 that the first-order bifurcation for a river channel is the first bifurcation that the channel undergoes (Fig.
270 4a). Although these methods were developed for deltaic channel networks, here we adapt them for fluvial
271 fan networks (Figs. 4c, 4d). We do not map or measure channels that loop or rejoin downstream, or

272 channels of non-fluvial origin, such as tidal channels or inlets (Smart, 1971; Tejedor et al., 2015) that are
273 not connected to the fluvial distributary channels. We also omit local avulsions on fluvial fans, which
274 generate channels that typically merge downfan (Slingerland and Smith, 2004). Paleo-channels on fluvial
275 fans were recorded where possible. Paleo-channels resembled active channels that exhibit little to no
276 discharge when we mapped the channel networks (Figs. 4c, 4d). We included paleo-channel
277 measurements in fluvial fans because they are ubiquitous in fluvial fans (Hartley et al., 2010), and many
278 of these channels do carry discharge if reactivated during major flood events.

279 **3.2 Channel Length and Width Measurements**

280 Channel length and width measurements follow Edmonds and Slingerland (2007), where channel
281 length is measured as the distance between two bifurcation nodes in deltas (Fig. 4a). We adopt this
282 methodology also to fluvial fans to measure channel lengths between avulsion nodes (Fig. 4c). The
283 average width of a channel segment is recorded from three separate width measurements: one
284 immediately after a node (w_i), one immediately before the next node (w_f), and one halfway between these
285 two points at the midpoint of the channel segment (w_h) (Figs. 4a, 4c). Land–water boundaries in both
286 deltas and fluvial fans were identified visually based on color (with water appearing darker and bluer than
287 land), surface texture, and vegetation contrast. In deltas, channel width measurements were recorded
288 based on the width of water present in the channel, which was nearly always delineated by clear
289 vegetation (Fig. 4b). For channels on fluvial fans, including paleo-channels, bankfull widths were
290 measured from clearly identifiable channel banks, vegetation patterns, and subtle depressions, allowing
291 for the mapping of dry or inactive channels (Fig. 4d). These approaches allowed measurement of inactive
292 channels while maintaining a uniform methodology and consistency for all width measurements. The
293 smallest measured channel widths resolvable in the imagery were 2-meter for deltas and 1-meter for
294 fluvial fans. Width measurements were not performed in locations where a channel has locally split into
295 multiple branches that join downstream.

296 Given the maximum 0.5-meter spatial resolution of the imagery (see Methods section 3.5), measuring
297 channels only a few meters wide carries some uncertainty. Normalization to the first-order channel width
298 helps mitigate this effect and reduce variability across systems. All channel width measurements were
299 normalized using the initial first-order channel width, following the methodology of Edmonds and
300 Slingerland (2007). Consequently, the normalized channel width value for first-order channels is always
301 equal to one. First-order channel lengths were measured between the last occurrence of tributary channels
302 and the first channel splitting node and contain no significant value for our study. Moreover, manual
303 digitization of fluvial fan channels spanning tens of kilometers may introduce minor inconsistencies in
304 channel path representation, particularly for narrow (<10 m) and highly sinuous channels. All channel
305 length measurements (l) were also normalized using the first-order channel width measurements

306 according to existing methodologies (Edmonds and Slingerland, 2007; Jerolmack, 2009), and this too
 307 helped to reduce uncertainties when digitizing channel lengths. As such, the normalized first-order
 308 channel length values merely reflect our selected methodologies rather than an attributable morphological
 309 characteristic.

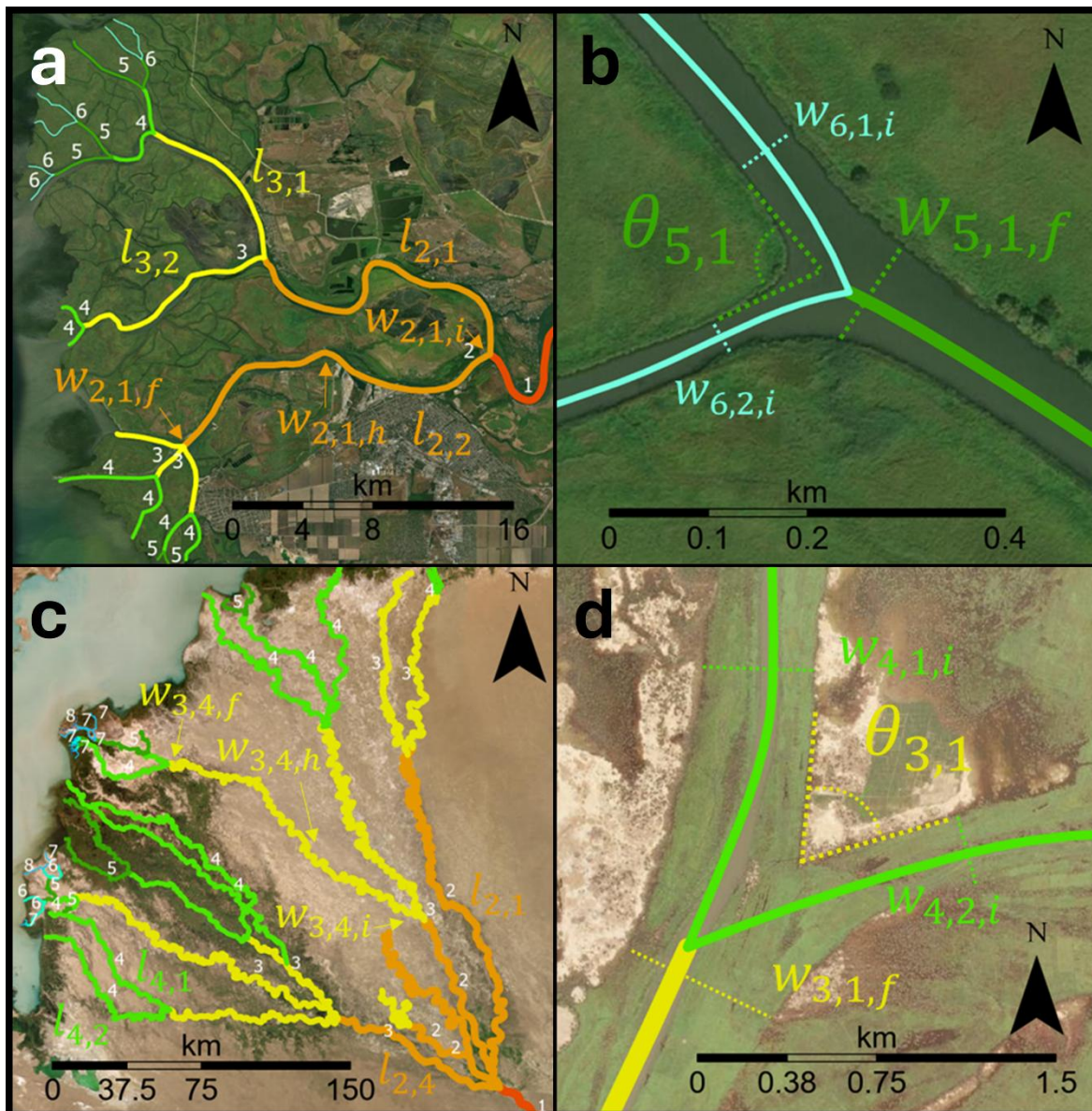


Figure 4: Illustration of (a) channel order, length, and width and (b) bifurcation angle measurements in deltas (Don delta). Illustration of (c) channel order, length, and width (Ili fan) and (d) divergence/crossover angle measurement (Niger fan). Arrows point to locations of w_i = initial channel width, w_h = midpoint channel width, w_f = final width measurements. The w_f is set as the length of two limbs that track along the edges of the mouth bar. θ_n corresponds to the bifurcation or divergence/crossover order. Base imagery from Esri's World Imagery basemap (© Esri, DigitalGlobe, GeoEye, i-cubed, USDA FSA, USGS, AEX, Getmapping, Aerogrid, IGN, IGP, swisstopo, and the GIS User Community).

311 3.3 Network Angle Measurements

312 To quantify network angles, we adopt the methodology of Coffey and Shaw (2017) developed for
313 measuring channel bifurcation angles, which determines the angles of mouth bars formed at the end of an
314 upstream channel. In this methodology, the final channel width directly upstream of a bifurcation (w_f) is
315 set as the length for two limbs of an angle that follows the mouth bar-water contact to measure a
316 bifurcation angle (θ_n) (Coffey and Shaw, 2017) (Fig. 4b). The same methodology is adapted here for
317 fluvial fans (Fig. 4d). In some river deltas, tidal processes cause bifurcation of a channel into three
318 channels instead of two; these are referred to as trifurcations (Leonardi et al., 2013), furcation (Shaw et
319 al., 2018), or polyfurcations (Chamberlain et al., 2018), and a few such measurements are included in the
320 dataset in the very distal portions of deltas where tidal influence is significant. We do not measure angles
321 where channels loop or rejoin downstream of avulsions or bifurcations. In essence, we focus on the
322 morphology of branching channel networks and measure the visible angles between channels or paleo-
323 channels independent of their origin (Figs. 4b, 4d).

324 3.4 Global Delta and Fluvial Fan Channel Network Database

325 To test the applicability of the proposed criteria, we selected 40 river-dominated deltas and 40
326 fluvial fans (Fig. 3 and Supplementary Data) to be mapped using composite satellite data (Esri, 2025).
327 These landforms were selected from a diverse range of hydroclimatic, topographic, and basinal conditions
328 from across the world (Fig. 3).

329 All deltas have been identified as such by prior work (Broaddus et al., 2022; Galloway, 1975;
330 Hartley et al., 2010; Leier et al., 2005; Nienhuis et al., 2015, 2018; Vulis et al., 2023), and they display
331 active discharge based on satellite imagery. Only river-dominated deltas are included in the dataset,
332 because wave-and tide-dominated delta morphology is distinct from that of fluvial fans. The river
333 dominance of deltas and the presence of tide- or wave-influence was determined using the established
334 principles of process-based delta classification (Broaddus et al., 2022; Galloway, 1975; Nienhuis et al.,
335 2015, 2018; Paniagua-Arroyave and Nienhuis 2024; Vulis et al., 2023). However, categorical
336 discrepancies exist between these different classification approaches. To clarify our terminology, we
337 define “dominated” versus “influenced” deltas as follows. Wave-dominated deltas (e.g. São Francisco,
338 Eel) are characterized by strandplains and a complete absence of bifurcations; these deltas are excluded
339 from our study. Wave-influenced deltas still possess morphological features such as strandplains, but
340 exhibit clear, measurable channel bifurcations and are included in our study. Similarly, tide-dominated
341 deltas (e.g. Fly, Yangtze) have a limited number of channels that widen substantially seaward, whereas
342 tide-influenced deltas such as the Yukon (Fig. 1c) exhibit channel widening only in the most distal
343 channels (Xu and Plink-Björklund, 2023). In practice, we combine these parameters with established
344 classifications (Broaddus et al., 2022; Galloway, 1975; Nienhuis et al., 2015, 2018; Paniagua-Arroyave

345 and Nienhuis, 2024; Vulis et al., 2023) to categorize the deltas in our study. Please refer to the
346 Supplementary Data for information regarding our classification of each delta. We test the effects of tide-
347 and wave-influence on the morphometric criteria by comparative analyses.

348 Fluvial fans were located using their apex coordinates from the global fluvial fan database of
349 Hartley et al. (2010). This database also includes data on fluvial fan length, gradient, termination style
350 (axial, contributory, lacustrine, marine, playa, desert/dune, and wetland). Termination styles refer to the
351 environment where the fluvial fan terminates: for instance, a contributory-termination style denotes that
352 the landform channels switch from distributary to contributory at the toe of the fan, while axial fans are
353 classified when the main channel forms a confluence with an axial fluvial system (Hartley et al., 2010).
354 Fluvial fans that enter oceans or lakes were originally distinguished from deltas based on (1) displaying
355 no significant modification of the planform by marine processes, such as wave or tidal influence; or (2)
356 the fluvial fans apex is close to the tidal limit (Hartley et al., 2010). They identified that on relatively
357 high-gradient systems (with slopes above 0.143°) marine reworking is normally restricted to the toe of the
358 fluvial fans and can be easily identified. On relatively low-gradient systems (with slopes below 0.0573°)
359 the influence of marine processes was more difficult to determine, and unless the landform apex was
360 located a significant distance inland (>200 km) the landform was excluded from their database. We added
361 a visual inspection that the channel network is a paleo-channel network, and we test the robustness of the
362 classification by comparative analyses of fluvial fans with lake and ocean terminations versus terrestrial
363 terminations. To further test the robustness of our methodology, we analyze whether the landform size,
364 gradient, termination style, or wave- and tide-influence in deltas affect the results.

365 **3.5 Mapping with ArcGIS Pro**

366 Delta and fluvial fan channel networks were mapped using ArcGIS Pro software (Version 3.2.1)
367 (Figs. 1, 2, and 4) with the ESRI World Imagery basemap, which provides up to 0.5-meter imagery for
368 most of the world (Esri, 2025). This resolution is suitable for mapping very narrow channels only several
369 meters wide. Alternative datasets such as Landsat (30-meter resolution) or Sentinel-2 (10-meter
370 resolution) are too coarse for this application; however they do contain multispectral bands that could be
371 useful in defining land-water contacts in places where it is ambiguous for wider channels. While ESRI
372 World Imagery is compiled from multiple providers and acquisition times, producing mosaicked tiles, we
373 did not observe noticeable changes in channel appearance across tile boundaries (e.g., abrupt changes in
374 channel width or discharge).

375 Another limitation of our dataset is uncertainty regarding the timing of satellite image acquisition
376 relative to precipitation events. Precipitation increases discharge, thereby increasing measured channel
377 widths, particularly for fluvial fans in arid environments. Such events can also reactivate partial avulsions
378 and crevasses, which can potentially increase the apparent number of channels. However, none of the

379 selected systems exhibited observable seasonal or large-scale discharge changes across their channel
380 networks attributable to different timings in data collection. Additionally, because this study relies on
381 values normalized to the initial channel width, the effects of seasonal variability on channel width
382 measurements are minimized.

383 Two feature classes were created: one for deltas and one for fluvial fans. Each delta or fluvial fan
384 landform was then individually mapped as a shapefile layer under the corresponding feature class
385 (Supplementary Data). The shapefiles for channel networks were created as polyline features, which
386 allow users to manually trace individual river channel segments while automatically recording line
387 lengths. Channel widths and angles were measured using the line and angle measurement tools in ArcGIS
388 Pro. All data were recorded in the attribute table for each landform. These data were organized into Excel
389 documents and subsequently converted to Python- and Pandas-readable CSV files (Supplementary Data).

390 **3.6 Code and Statistics**

391 Kolmogorov-Smirnov (KS) and Shapiro-Wilk (SW) tests were first applied to determine whether
392 the data are normally distributed. Levene's test was used to test differences in variances of populations
393 that do not exhibit a normal distribution (Trauth, 2006). Independent sample t-test or Welch's t-test were
394 then applied to test for a difference in means for populations with similar and dissimilar variances,
395 respectively, while one-sample t-tests were used to test comparisons of a subgroup against the overall
396 population mean (Trauth, 2006). For this study, a p-value less than 0.05 (5% significance level) suggests
397 that the two population distributions, variances, or means are not similar. Data confidence intervals were
398 calculated according to Mendenhall et al. (2012). Data analysis and visualization were performed using
399 Python. Open-source data visualization libraries Matplotlib (Hunter, 2007), NumPy (Harris et al., 2020),
400 SciPy (Virtanen et al., 2020), and Seaborn (Waskom, 2021) were utilized.

401 **4. Results**

402 **4.1 Delta and Fluvial Fan Channel Network Angles**

403 The mean channel network angle (θ_d) in deltas is 74.0° with a 95th percentile confidence interval of \pm
404 1.9° ($n = 527$) (Fig. 5a). The mean channel network angle (θ_f) in fluvial fans is $55.0^\circ \pm 2.0^\circ$ ($n = 520$)
405 (Fig. 5b). The delta and fluvial fan network angle populations are not normally distributed according to
406 both Kolmogorov-Smirnov and Shapiro-Wilk tests, with p-values less than 0.05. Levene's test for
407 statistical difference in variances also results in a p-value less than 0.05, suggesting population variances
408 are statistically different. A subsequent independent sample t-test suggests the means of delta and fluvial
409 fan angle populations are statistically different, with a p-value less than 0.05. All statistical results are
410 recorded in Supplementary Table 1 in the Supplementary Information.

411 We also reviewed the mean network angle of each individual delta and fluvial fan (θ_{Landform}) (Figs. 5c,
412 5d), and these analyses reveal some overlap. All fluvial fans have mean angle values less than 60° , except

413 for six landforms, or 15% of fluvial fans in this study. Four of these landforms have mean angles larger
 414 than 60° (60.8° , 63.2° , 67.7° , 67.9°), and two larger than the delta mean of 73.7° (79.6° , 80.1°). All
 415 individual deltas have mean network angles larger than 60° , except for one delta (59.3°). There are also
 416 three deltas with mean angles around 60° (61.5° , 62.4° , 63.3°).

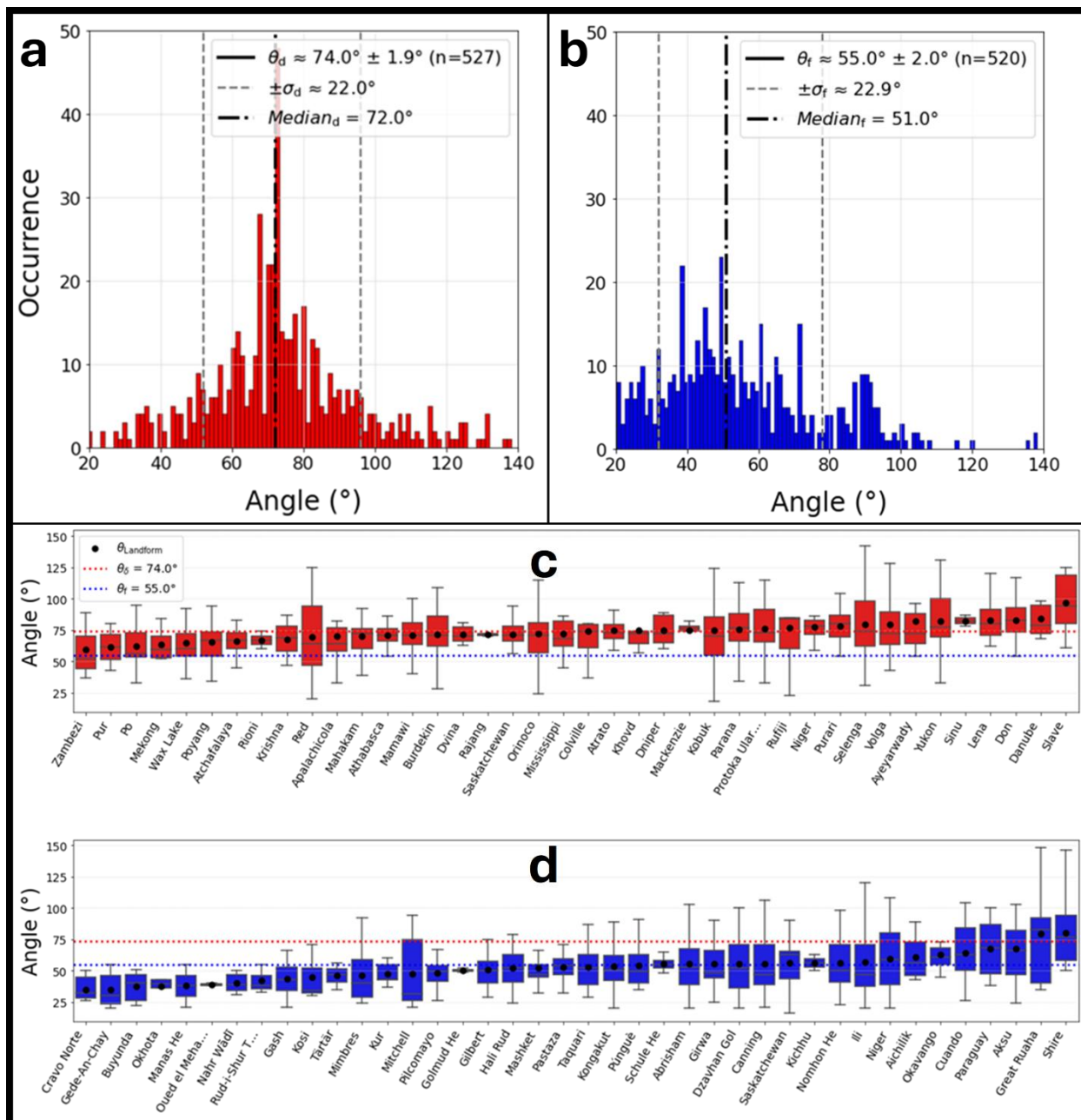


Figure 5: Histograms depicting distributions of (a) delta channel network angles with mean angle (θ_d), its standard deviation (σ_d) and median, and (b) fluvial fan channel network angles with mean fan angle (θ_f), its standard deviation (σ_f) and median. Box-and-whisker plots with the mean angle for each delta (c) and fluvial fan (d) landform ($\theta_{Landform}$).

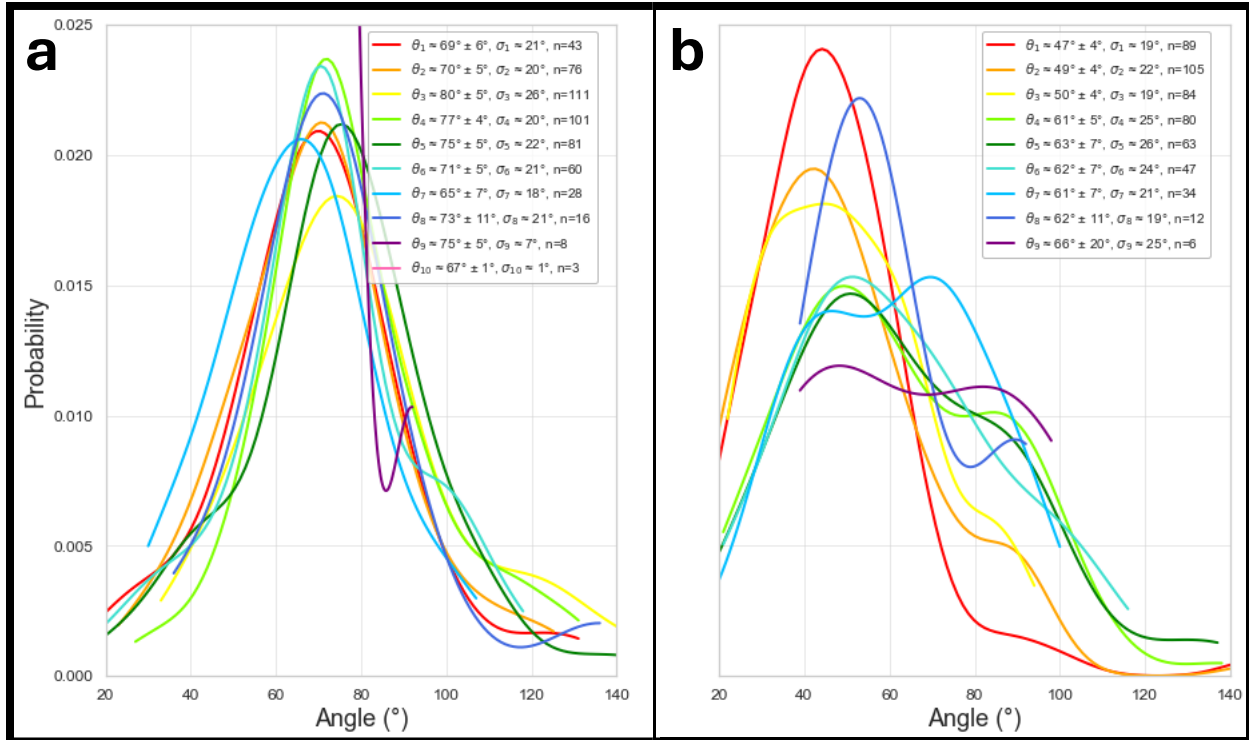


Figure 6: Distribution of (a) delta, and (b) fluvial fan network angles grouped by order (θ_n) with the 95th percent confidence interval. (σ_n) = denotes standard deviation. n denotes sample size.

417 The distribution of delta angles grouped by order (Fig. 6a) yields no strong trends for mean angle in
 418 deltas. Seventh and tenth order channels have slightly lower mean angle values at 65° and 67°, but these
 419 higher-order groups have low sample sizes (n = 3; n = 8) (Fig. 6a). The distribution of fluvial fan angles
 420 grouped by order does yield a trend: the mean angle for first- through third-order channels (θ_1 , θ_2 , and θ_3
 421 in Fig. 6b) is between 47–50° and increases to 61–63° for fourth- through eighth-order channels, and to
 422 66° for ninth-order angles (n = 6) (θ_4 – θ_9 in Fig. 6b). In contrast to the unimodal distribution of delta
 423 angles, the distribution of higher-order fluvial fan angles is bimodal, with a dominant peak near 50° and a
 424 secondary peak around 80–100° (Fig. 6b).

425 All deltas in this analysis are river-dominated deltas, however some are tide- or wave-influenced (see
 426 Section 3.4 and Supplementary Data). Grouping deltas by process regime shows that the mean network
 427 angle for the 19 river-dominated deltas ($\theta_R = 73.6^\circ \pm 2.2^\circ$, n = 374), for the 16 tide-influenced deltas ($\theta_t =$
 428 $75.6^\circ \pm 3.9^\circ$, n = 139), and for the 5 wave-influenced deltas ($\theta_w = 67.1^\circ \pm 10.1^\circ$, n = 14) (Fig. 7a). The
 429 river-dominated and tide-influenced delta angle means are not statistically different from the mean angle
 430 for the whole delta population (Supplementary Table 1). The wave-influenced delta angles were omitted
 431 from this statistical analysis due to a small sample size (n = 14 < 30).

432 Many delta angle measurements in this dataset come from Arctic deltas. The comparison between
 433 Arctic and non-Arctic deltas shows that Arctic deltas have a larger mean angle ($\theta_A = 76.5^\circ \pm 2.7^\circ$, n =

434 263) than non-Arctic deltas ($\theta_{NA} = 71.4^\circ \pm 2.6^\circ$, $n = 264$) (Fig. 7b). There is a statistically significant
 435 difference in means between Arctic and non-Arctic deltas (Supplementary Table 1). Grouping deltas by
 436 termination style (Fig. 7c) shows that lake-terminating deltas have slightly smaller mean angles than those
 437 that terminate in oceans ($\theta_L = 72.9^\circ \pm 3.2^\circ$, $n = 160$, versus $\theta_O = 74.4^\circ \pm 2.3^\circ$, $n = 367$), but these
 438 differences are not statistically significant compared to the whole delta population (Supplementary Table
 439 1).

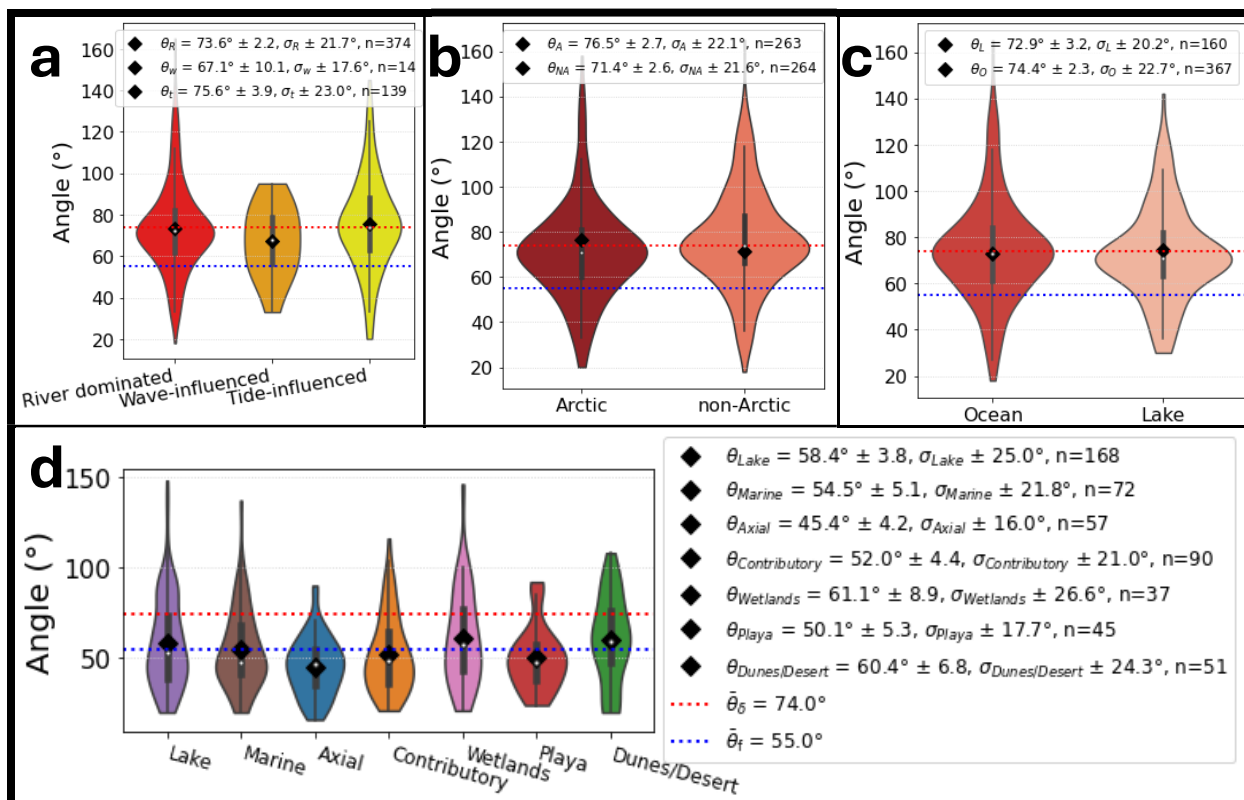


Figure 7: Violin plots depicting network angle distributions by (a) delta process regime: river dominated (θ_R), wave-influenced (θ_W), and tide-influenced (θ_T), (b) deltas in non-Arctic (θ_{NA}) and Arctic (θ_A) climates, (c) ocean terminating deltas (θ_O) and lake terminating deltas (θ_L), and (d) fluvial fan termination styles. All mean angle values have a corresponding 95th percent confidence interval, standard deviation (σ), and sample count (n).

440
 441 Grouping fluvial fans by their termination style shows some differences (Fig. 7d), where the mean
 442 angles vary from a low of $\theta_{Axial} = 45.4^\circ \pm 4.2^\circ$ ($n = 57$) for axial-terminating fluvial fans to $\theta_{wetlands} = 61.1^\circ$
 443 $\pm 8.9^\circ$ ($n = 37$) for wetland-terminating fans (Fig. 7d). All fluvial fan termination types, except for axial-
 444 terminating fans, exhibit population means that are statistically similar to the overall fluvial fan
 445 population (Supplementary Table 1). However, each termination style is represented by only 4 to 6
 446 landforms, limiting the statistical power of comparisons and generalizations, despite the relatively robust
 447 measurement numbers in wetland ($n = 37$), playa ($n = 45$), dunes/desert ($n = 51$), and axial-terminating

448 fans ($n = 57$). There also appears to be some discrepancies in Hartley et al. (2010)'s assignment of
449 termination types, such as referring to playa fans as lacustrine or ocean fans as contributory. We also
450 tested whether landform size (Supplementary Fig. 1) and gradient (Supplementary Fig. 2) affect the
451 channel network angles, and these analyses yield no trends, supporting the robustness of our
452 methodology.

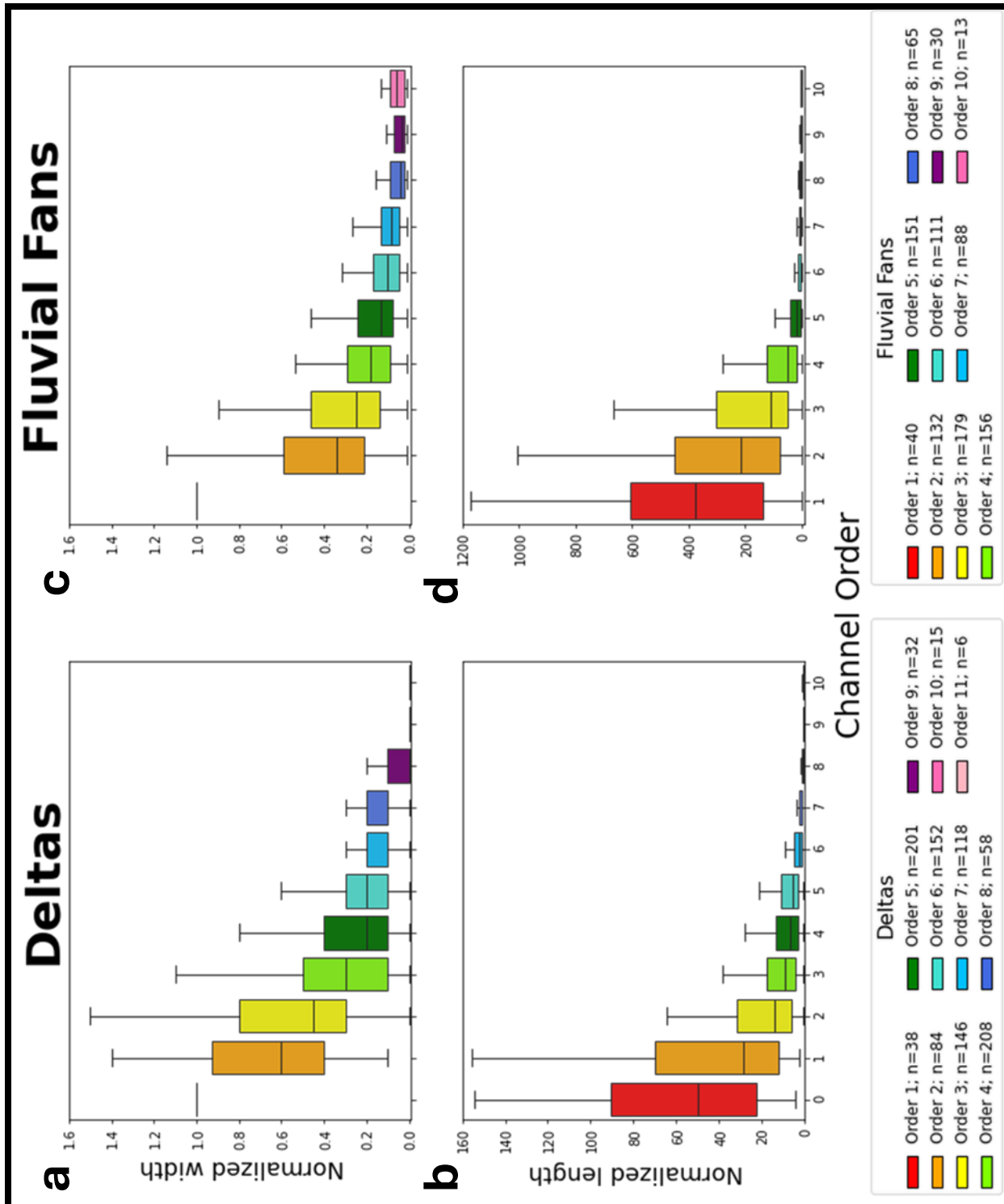
453 **4.2 Channel Lengths and Widths**

454 Normalized channel length and width measurements reveal morphological differences between
455 fluvial fan and delta channels. Both landform types show non-linear decreases in these values with
456 increasing channel order (Fig. 8). Statistical analyses confirm that the overall means for normalized
457 channel length and width differ significantly between fluvial fans and deltas (Supplementary Table 1).
458 Fluvial fan channels are generally an order of magnitude longer than delta channels, with a mean
459 normalized length of 147.09 compared to 17.18 for deltas (Figs. 8a, 8c). In contrast, delta channels tend to
460 be slightly wider, with a mean normalized width of 0.40 compared to 0.26 for fluvial fans (Figs. 8b, 8d).

461 Comparing the normalized dimensions by channel order (Fig. 9) reveals additional trends. The
462 normalized channel lengths of lower-order fluvial fan channels (orders 1–5) are significantly longer, and
463 the channel shortening rate is higher compared to deltas (Fig. 9a). The normalized lengths become very
464 similar in orders 7–8, then diverge again for the higher orders where the fluvial fan channel lengths are
465 somewhat longer, but the channel shortening rates are higher in deltas. Normalized channel widths show
466 significant differences for orders 2–8, but not for 9–11. Only a few landforms have channels with orders
467 exceeding 9. Fluvial fan narrowing rates are very high from orders 1 and 2, and very low in orders 7–10
468 (Fig. 9b). The narrowing rates are more uniform in deltas. When comparing individual deltas by process
469 regime, both tide- and wave-influenced deltas have significantly higher mean normalized channel widths
470 relative to the overall delta population (Supplementary Fig. 3 and Supplementary Table 1).

471 Comparison by fluvial fan termination styles shows that axial- and playa-terminating fans exhibit
472 longer mean normalized channel lengths compared to the whole fluvial fan population, whereas
473 dunes/desert-, marine-, and wetland-terminating fans have shorter mean lengths (Supplementary Fig. 3
474 and Supplementary Table 1). Contributory- and lake-terminating fans do not differ significantly from the
475 overall mean. Regarding normalized channel widths, axial- and marine-terminating fans have wider
476 channels, while dunes/desert-terminating fans are narrower. Normalized width values for contributory-,
477 lake-, playa-, and wetland-terminating fan channels show no difference from the overall population mean
478 (Supplementary Fig. 3 and Supplementary Table 1). Statistical analyses of channel length and width were
479 not conducted for different fluvial fan termination styles due to insufficient sample sizes ($n < 30$) in most
480 categories.

481



482 Figure 8: Box and whisker plots illustrating normalized delta channel widths (a) and lengths (b), and normalized fluvial fan channel widths (c) and lengths (d), plotted by channel order. Note the significant difference in normalized channel length scales for subplots b and d.

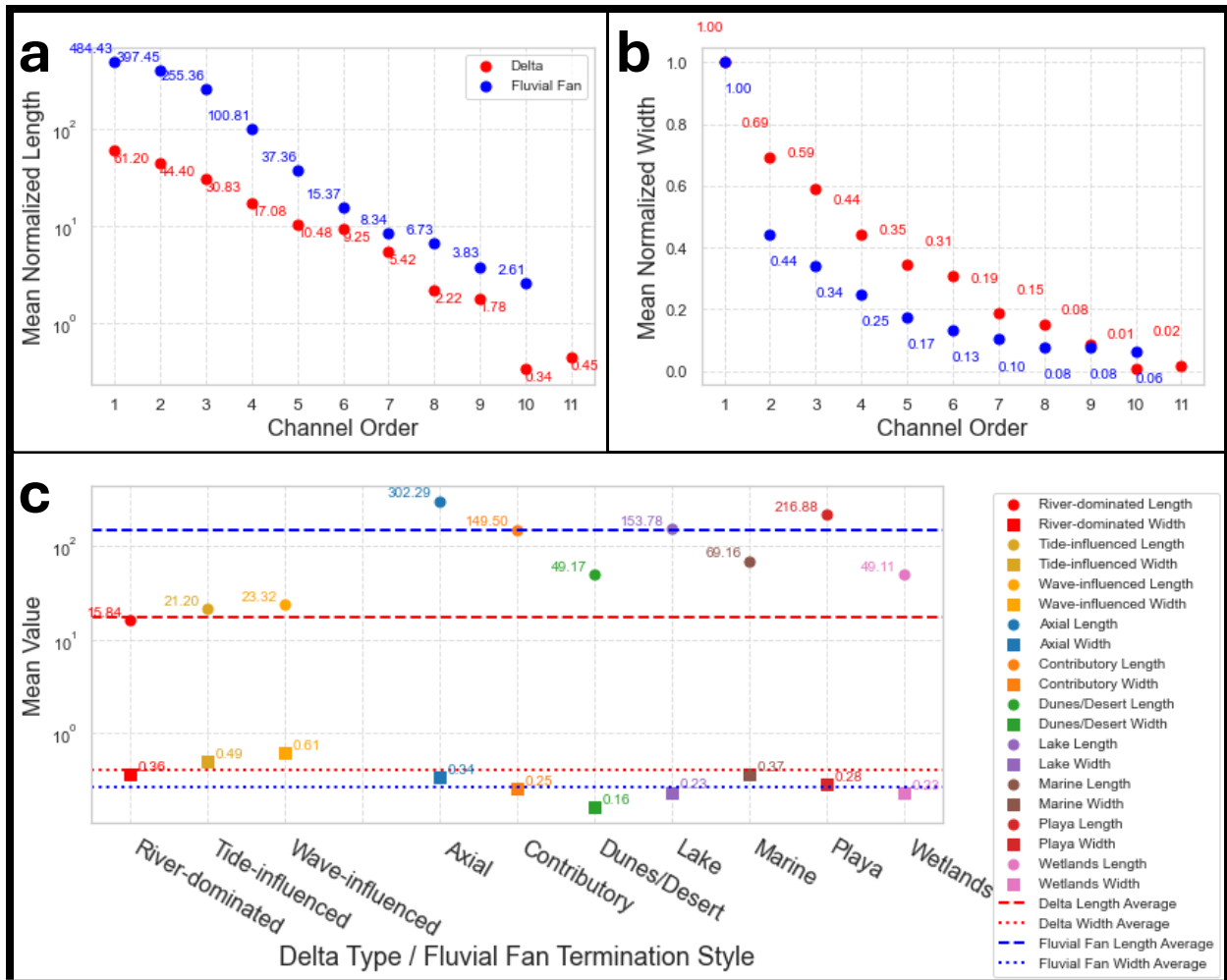


Figure 9: Mean normalized delta and fluvial fan channel (a) length and (b) width values by order. (c) Mean channel length and width values for different types of deltas and fluvial fan termination styles.

483

484 **5. Discussion**

485 **5.1 Effectiveness of Morphometric Criteria in Distinguishing Deltas and Fluvial Fans**

486 The mean channel network angles are distinctly different in deltas and fluvial fans by 20°, and this
 487 statistically significant difference is a useful criterion in distinguishing these two landform types. While
 488 some overlaps exist at the landform level, these cases are relatively limited, where 15% of fluvial fans in
 489 this dataset have a mean angle larger than 60° (Fig. 5d) and 10% of deltas have a mean angle less than
 490 64° (Fig. 5c). These findings support the utility of mean branching angles as a distinguishing metric
 491 between deltas and fluvial fans. However, some degree of uncertainty remains, and additional criteria are
 492 necessary for more robust distinction.

493 An additional criterion is the distribution of mean angles by channel order, where fluvial fans have
 494 increased mean angles and a bimodal distribution in orders 4–8 (Fig. 6). Other supportive criteria may be

495 the differences in values and distributions of the normalized channel lengths and widths (Figs. 8 and 9),
496 but the low sample numbers do not allow us to test these criteria by individual landforms. A useful
497 criterion would be to link channel narrowing with the bifurcation and avulsion nodes. In deltas, the
498 downstream channel narrowing occurs in a stepwise manner at the mouth-bar-driven bifurcation nodes,
499 whereas in fluvial fans this decrease should be gradual and not linked to the node positions where full
500 avulsions occur. Our data were collected in a manner that does not permit these analyses.

501 A potential source of overlap in the delta and fluvial fan channel network mean angles is that not all
502 measured angles in deltas are mouth-bar-driven bifurcation angles, as deltas also experience avulsions
503 (e.g., Fig. 1h). A closer inspection of the four deltas with low mean network angles reveals that each
504 contains very few measurements ($n = 3$, $n = 4$, $n = 6$, $n = 7$). In these cases, the limited sample size allows
505 the rarer avulsion angles to affect the mean values more strongly. Also, fluvial fans that terminate in a
506 lake or ocean may have terminal channels that form due to mouth bar deposition and channel bifurcation.
507 However, we do not believe these instances affect our results, since we do not see that lake- or marine-
508 terminating fans exhibit higher mean angles (Fig. 7d).

509 Examining fluvial fans with high mean angles shows that these are low-gradient wetland fans, where
510 the avulsion angles tend to be wider as a function of avulsion mechanisms (see Discussion below).
511 However, they may also suggest methodological limitations. While the local avulsion angles in low-
512 gradient wetland fans are wide (using the final channel width directly upstream of a branching node (w_f)
513 as the length for two limbs of an angle; Fig. 4b), angles between the longer channel reaches are
514 considerably narrower (Supplementary Fig. 4). This channel reach angle discrepancy is consistent with
515 similar channel reach angle measurements from Coffey and Shaw (2017). We plan to further develop
516 angle measurement methods to capture both the local and the reach-scale angles in future work. It is also
517 important to discuss the limitations of the applied methodologies in the context of the results. Our channel
518 network methodologies are designed for delta channel networks, and exclude channels that merge
519 downstream, which can exclude many potential measurements from fluvial fans in situations where their
520 channels merge downfan.

521 In summary, this initial attempt to distinguish deltas and fluvial fans demonstrates that quantifying
522 channel network angles, and trends in normalized channel widths and lengths provide efficient criteria.
523 However, we also show that sample sizes are important for accurate recognition of landforms, and
524 collecting a sufficient number of angle measurements ($n \gtrsim 10$) can help account for the infrequent
525 avulsion in deltas or bifurcation in fluvial fans. While each metric is informative on its own, the
526 combination of branching angles, branching angle trends, and normalized channel lengths provides the
527 clearest distinction between deltas and fluvial fans.

528

529 **5.2 Processes that determine delta and fluvial fan channel network angles**

530 While the 72° mean mouth-bar-driven bifurcation angle is linked to flow patterns at channel tips well-
531 explained by diffusive processes (Coffey and Shaw, 2017), there is currently no established explanation
532 for the approximately 55° mean network angle in fluvial fans. In deltas, mouth-bar-driven bifurcation is
533 the product of sedimentation from turbulent jets that form at the mouths of rivers entering basins (Bates,
534 1953; Coffey and Shaw, 2017; Edmonds and Slingerland, 2007; Fagherazzi et al., 2015; Jerolmack and
535 Swenson, 2007; Wright, 1977). Once a mouth bar is formed, the flow through the distributary channel
536 bifurcations can be modeled as diffusive flow (Coffey and Shaw, 2017), and the resulting critical angle of
537 72° represents a stable morphology for the bifurcation as it grows in a diffusive groundwater field
538 (Devauchelle et al., 2012; Ke et al., 2019). The slightly larger network angles in Arctic deltas may reflect
539 environmental influences such as ice cover, permafrost, or limitations on overbank flow (Lauzon et al.,
540 2019; Piliouras et al., 2021; Walker, 1998).

541 River avulsions are set up by channel superelevation (Mohrig et al., 2000), or when the slope down
542 the flanks of the channel provides a steeper descent than the existing river channel (Slingerland and
543 Smith, 1998; Törnqvist and Bridge, 2002). Avulsions result from channel bed aggradation that reduces
544 the channel capacity (Bryant et al., 1995). Once an avulsion is triggered and full or partial river flow exits
545 the channel, a new channel is generated by surface runoff erosion. Thus, the prevailing topographic
546 gradient would tend to keep the nearby flows more focused in a slope-parallel direction, resulting in
547 narrower network angles compared to mouth-bar-driven bifurcations (Fig. 5b).

548 The contrast between diffusion-dominated and surface runoff erosion-dominated processes in shaping
549 delta versus fluvial fan channel network topology is further supported by tributary channel network
550 analyses that originally defined the critical angle of 72° (Devauchelle et al., 2012). Tributary channel
551 network analyses show that the mean tributary angle of 72° only occurs in humid catchments with high
552 groundwater recharge, where tributary networks are shaped by groundwater diffusion (Seybold et al.,
553 2017). In contrast, the mean tributary network angle is 45° in arid landscapes where surface runoff
554 dominates (Seybold et al., 2017), or is even lower in the driest catchments (Seybold et al., 2018).

555 Fluvial fan gradient decreases progressively downstream (e.g. Chakraborty et al., 2010), such that
556 higher gradients near the fan apex likely generate more acute angles, whereas the very low gradients near
557 the toe of the fan would allow for wider angles. This trend likely explains the downstream increase in
558 fluvial fan network angles and the emergence of the second, wider peak in higher order channels (Fig.
559 6b). Furthermore, avulsion mechanisms have been shown to change from channel superelevation in
560 upstream river reaches, where river gradients are steeper, to gradient advantage in downstream low-
561 gradient reaches (Gearon et al., 2024). In these low-gradient zones, crevassing processes can produce
562 high-angle deviations with the angle values around 90° (Rahman et al., 2022). Avulsion angles above

563 100° have been measured in meandering rivers on low-gradient floodplains with vegetation (see Rahman
564 et al., 2022). These effects may be important controls in the fluvial fan channel networks in low-gradient
565 vegetated wetlands. Reitz and Jerolmack (2012) show that abandoned paleo-channel reoccupation may
566 control new avulsion positions, and paleo-channel density is highest in the narrower fan apex. Avulsion
567 angles may also change over time due to evolving channel width ratios (Morais and Montanher, 2022), or
568 may be affected by a critical angle or bend curvature (Yang, 2020). Future work targeting how avulsion
569 morphology evolves downfan would provide important insight into the mechanisms driving the observed
570 increase in angles downstream.

571 We thus conclude that the distinction between deltaic and fluvial fan channel network angles arises
572 from the dominant formative processes: diffusive flow in deltas versus surface runoff erosion in fluvial
573 fans. Furthermore, in fluvial fans, network angles appear to be negatively correlated with surface
574 gradients, with lower gradients allowing for wider avulsion angles.

575 **5.3 Ancient deltas and fluvial fans**

576 Our proposed methodology could also be used to distinguish ancient fluvial fans and deltas, for
577 instance in seismic datasets, where only delta channel network angles have been quantified before
578 (Mahon et al., 2024). Our results confirm the prior modern data (Chakraborty et al., 2010) and recent
579 modeling outcomes (Martin and Edmonds, 2023), and help to eliminate a discrepancy in plan-view versus
580 cross-sectional fluvial fan facies models (Plink-Björklund, 2021). Namely, earlier work suggested
581 processes similar to mouth-bar-driven bifurcations as a key mechanism driving fluvial fan formation
582 (Friend, 1978; Kelly and Olsen, 1993; Weissmann et al., 2010), probably due to downstream channel
583 narrowing. However, this hypothesis contradicts the stratigraphic data that indicate that proximal fans
584 consist of amalgamated channel deposits (Chakraborty et al., 2010; Kelly and Olsen, 1993; Nichols and
585 Fisher, 2007; Singh et al., 1993; Weissmann et al., 2013) – a pattern consistent with frequent avulsions
586 (Chakraborty et al., 2010; Singh et al., 1993).

587 **5.4 Sensitivity of Deltas and Fluvial Fans to Global Change**

588 Deltas and fluvial fans differ significantly in their vulnerability to natural hazards and in their
589 responses to global change. Deltas are highly vulnerable to coastal hazards and sea-level rise (Giosan et
590 al., 2014; Syvitski et al., 2009). Rising sea-levels will not only inundate deltaic distributary networks, but
591 also cause a landward migration of the avulsion node corresponding with the landward shift of the
592 backwater zone (Brooke et al., 2022; Chatanantavet et al., 2012; Ganti et al., 2014). This process reduces
593 sediment delivery to shorelines, accelerating the effects of sea-level rise. However, changes in land use
594 and changing precipitation patterns which increase sediment supply could complicate the picture by
595 shifting delta avulsion sites seaward (Brooke et al., 2022). In contrast, fluvial fans are controlled by
596 upstream morphodynamics, where the fan location (apex) is pinned by a steep topographic break (Brooke

597 et al., 2022; Ganti et al., 2014; Martin and Edmonds, 2023). For coastal fans, sea-level rise and coastal
598 erosion would affect the fan toes, however the avulsion node at the fan apex and sediment deposition
599 across most of the fan surface would not be affected, making fluvial fans significantly less vulnerable to
600 sea-level rise.

601 Both deltas and fluvial fans are affected by reduced sediment supply due to river damming and
602 artificial levees (Blum and Roberts, 2009; Giosan et al., 2014; Nienhuis et al., 2020; Paola et al., 2011;
603 Syvitski et al., 2009). However, fluvial fans are highly sensitive to the water and sediment supply
604 changes, such as changes in precipitation patterns (Assine et al., 2014; Hansford and Plink-Björklund,
605 2020; Leier et al., 2005). Increases in extreme precipitation cause a significant increase in avulsion
606 frequency and crevassing splay formation (Morón et al., 2017), because large fluctuations in river
607 discharge, such as during extreme precipitation events, are avulsion-triggering events (Jones and
608 Schumm, 1999). Indeed, fluvial fans have been shown to be highly sensitive to such changes, where
609 fluvial fan activation and deactivation cycles have been linked to millennial-scale changes in monsoon
610 intensity or precipitation patterns (Assine et al., 2014; Fontana et al., 2014; Latrubesse et al., 2012).

611 **6. Conclusions**

612 This study demonstrates that river-dominated delta and fluvial fan channel networks can be
613 distinguished using quantitative morphometric criteria derived from their channel network topology.
614 Deltaic networks are primarily shaped by mouth-bar-driven bifurcation processes, resulting in mean
615 bifurcation angles of approximately 74° , consistent with diffusion-dominated growth. In contrast, fluvial
616 fan topology is shaped by channel avulsions, producing narrower mean network angles near 55° ,
617 indicative of surface runoff processes. Fluvial fan network angles tend to widen downstream, likely due to
618 decreasing gradients and avulsion style shifts, while delta angles remain relatively consistent, reflecting
619 persistent mouth-bar-driven bifurcation processes. Both channel networks display downstream reductions
620 in channel length and width with increasing channel order, but the fluvial fan networks are characterized
621 by significantly longer and somewhat narrower channels when normalized.

622 These differences not only support the use of network morphology as a diagnostic tool for identifying
623 ancient fluvial fans and deltas in the stratigraphic record or other planetary bodies but also provide
624 insights into their differing sensitivities to environmental change.

625

626 **Code Availability**

627 The Python code used for data analysis and figure generation was created and run in Jupyter Notebook
628 version 6.4.8 (Anaconda distribution).

629

630

631 **Data Availability**

632 Morphological data collected in this study are available at [https://github.com/lukegezovich/Delta-and-](https://github.com/lukegezovich/Delta-and-Fluvial-Fan-Networks)
633 [Fluvial-Fan-Networks](https://github.com/lukegezovich/Delta-and-Fluvial-Fan-Networks).

634

635 **Author Contribution**

636 LG was responsible for the investigation and data curation, development of methodology, formal analysis
637 and visualization, and writing the original draft of the manuscript. PPB initiated the project, co-developed
638 the initial methodology, and co-wrote the manuscript. JH co-developed the initial methodology and
639 perform initial mapping and analyses of a small number of systems.

640

641 **Competing Interests**

642 The authors declare that they have no conflict of interest.

643

644 **Acknowledgments**

645 We thank Kamini Singha, Lesli Wood, and Wendy Zhou for their constructive feedback that helped
646 improve earlier versions of this manuscript. We also thank John Shaw, Ellen Chamberlin, Anastasia
647 Piliouras, and an anonymous reviewer for their helpful comments on the present versions of the
648 manuscript.

649

650 **Financial Support**

651 Luke Gezovich thanks the American Association of Petroleum Geologists (AAPG) Foundation John &
652 Erika Lockridge Grant, the American Institute of Professional Geologists (AIPG) William J. Siok Graduate
653 Scholarship, the Colorado Scientific Society (CSS), the Rocky Mountain Association of Geologists
654 (RMAG), and the Society for Sediment Geology (SEPM) for providing funding to support this research.

655

656 **References**

657 Allen, P. A.: Time scales of tectonic landscapes and their sediment routing systems, *SP*, 296, 7–28,
658 <https://doi.org/10.1144/SP296.2>, 2008.

659 Assine, M. L.: River avulsions on the Taquari megafan, Pantanal wetland, Brazil, *Geomorphology*, 70,
660 357–371, <https://doi.org/10.1016/j.geomorph.2005.02.013>, 2005.

661 Assine, M. L., Corradini, F. A., Pupim, F. D. N., and McGlue, M. M.: Channel arrangements and
662 depositional styles in the São Lourenço fluvial megafan, Brazilian Pantanal wetland, *Sedimentary*
663 *Geology*, 301, 172–184, <https://doi.org/10.1016/j.sedgeo.2013.11.007>, 2014.

664 Axelsson, V.: The Laitaure Delta: A Study of Deltaic Morphology and Processes, *Geografiska Annaler*.
665 Series A, Physical Geography, 49, 1, <https://doi.org/10.2307/520865>, 1967.

- 666 Bates, C. C.: Rational Theory of Delta Formation, *Bulletin*, 37, <https://doi.org/10.1306/5CEADD76-16BB-11D7-8645000102C1865D>, 1953.
- 668 Bentley, S. J., Blum, M. D., Maloney, J., Pond, L., and Paulsell, R.: The Mississippi River source-to-sink
669 system: Perspectives on tectonic, climatic, and anthropogenic influences, Miocene to Anthropocene,
670 *Earth-Science Reviews*, 153, 139–174, <https://doi.org/10.1016/j.earscirev.2015.11.001>, 2016.
- 671 Blair, T. C. and McPherson, J. G.: Alluvial Fans and their Natural Distinction from Rivers Based on
672 Morphology, Hydraulic Processes, Sedimentary Processes, and Facies Assemblages, *SEPM JSR*, Vol.
673 64A, <https://doi.org/10.1306/D4267DDE-2B26-11D7-8648000102C1865D>, 1994.
- 674 Blum, M. D. and Roberts, H. H.: Drowning of the Mississippi Delta due to insufficient sediment supply
675 and global sea-level rise, *Nature Geosci*, 2, 488–491, <https://doi.org/10.1038/ngeo553>, 2009.
- 676 Bramble, M. S., Goudge, T. A., Milliken, R. E., and Mustard, J. F.: Testing the deltaic origin of fan
677 deposits at Bradbury Crater, Mars, *Icarus*, 319, 363–366, <https://doi.org/10.1016/j.icarus.2018.09.024>,
678 2019.
- 679 Broaddus, C. M., Vulis, L. M., Nienhuis, J. H., Tejedor, A., Brown, J., Foufoula-Georgiou, E., and
680 Edmonds, D. A.: First-Order River Delta Morphology Is Explained by the Sediment Flux Balance From
681 Rivers, Waves, and Tides, *Geophysical Research Letters*, 49, <https://doi.org/10.1029/2022GL100355>,
682 2022.
- 683 Brooke, S., Chadwick, A. J., Silvestre, J., Lamb, M. P., Edmonds, D. A., and Ganti, V.: Where rivers
684 jump course, *Science*, 376, 987–990, <https://doi.org/10.1126/science.abm1215>, 2022.
- 685 Bryant, M., Falk, P., and Paola, C.: Experimental study of avulsion frequency and rate of deposition,
686 *Geol*, 23, 365, [https://doi.org/10.1130/0091-7613\(1995\)023%253C0365:ESOFAFA%253E2.3.CO;2](https://doi.org/10.1130/0091-7613(1995)023%253C0365:ESOFAFA%253E2.3.CO;2), 1995.
- 687 Chakraborty, T., Kar, R., Ghosh, P., and Basu, S.: Kosi megafan: Historical records, geomorphology and
688 the recent avulsion of the Kosi River, *Quaternary International*, 227, 143–160,
689 <https://doi.org/10.1016/j.quaint.2009.12.002>, 2010.
- 690 Chamberlain, E. L., Törnqvist, T. E., Shen, Z., Mauz, B., and Wallinga, J.: Anatomy of Mississippi Delta
691 growth and its implications for coastal restoration, *Sci. Adv.*, 4, eaar4740,
692 <https://doi.org/10.1126/sciadv.aar4740>, 2018.
- 693 Chatanantavet, P. and Lamb, M. P.: Sediment transport and topographic evolution of a coupled river and
694 river plume system: An experimental and numerical study: EXPERIMENTS COUPLED RIVER &
695 RIVER-PLUME, *J. Geophys. Res. Earth Surf.*, 119, 1263–1282, <https://doi.org/10.1002/2013JF002810>,
696 2014.
- 697 Chatanantavet, P., Lamb, M. P., and Nittrouer, J. A.: Backwater controls of avulsion location on deltas,
698 *Geophysical Research Letters*, 39, 2011GL050197, <https://doi.org/10.1029/2011GL050197>, 2012.
- 699 Chen, C., Tian, B., Schwarz, C., Zhang, C., Guo, L., Xu, F., Zhou, Y., and He, Q.: Quantifying delta
700 channel network changes with Landsat time-series data, *Journal of Hydrology*, 600, 126688,
701 <https://doi.org/10.1016/j.jhydrol.2021.126688>, 2021.
- 702 Coffey, T. S. and Shaw, J. B.: Congruent Bifurcation Angles in River Delta and Tributary Channel
703 Networks, *Geophysical Research Letters*, 44, <https://doi.org/10.1002/2017GL074873>, 2017.

- 704 Davidson, S. K. and Hartley, A. J.: A Quantitative Approach To Linking Drainage Area and Distributive-
705 Fluvial-System Area In Modern and Ancient Endorheic Basins, *Journal of Sedimentary Research*, 84,
706 1005–1020, <https://doi.org/10.2110/jsr.2014.79>, 2014.
- 707 Davidson, S. K., Hartley, A. J., Weissmann, G. S., Nichols, G. J., and Scuderi, L. A.: Geomorphic
708 elements on modern distributive fluvial systems, *Geomorphology*, 180–181, 82–95,
709 <https://doi.org/10.1016/j.geomorph.2012.09.008>, 2013.
- 710 De Toffoli, B., Plesa, A. -C., Hauber, E., and Breuer, D.: Delta Deposits on Mars: A Global Perspective,
711 *Geophysical Research Letters*, 48, e2021GL094271, <https://doi.org/10.1029/2021GL094271>, 2021.
- 712 Devauchelle, O., Petroff, A. P., Seybold, H. F., and Rothman, D. H.: Ramification of stream networks,
713 *Proc. Natl. Acad. Sci. U.S.A.*, 109, 20832–20836, <https://doi.org/10.1073/pnas.1215218109>, 2012.
- 714 Di Achille, G. and Hynek, B. M.: Ancient ocean on Mars supported by global distribution of deltas and
715 valleys, *Nature Geosci*, 3, 459–463, <https://doi.org/10.1038/ngeo891>, 2010.
- 716 Dong, T. Y., Nittrouer, J. A., Il'icheva, E., Pavlov, M., McElroy, B., Czapiga, M. J., Ma, H., and Parker,
717 G.: Controls on gravel termination in seven distributary channels of the Selenga River Delta, Baikal Rift
718 basin, Russia, *Geological Society of America Bulletin*, 128, 1297–1312,
719 <https://doi.org/10.1130/B31427.1>, 2016.
- 720 Donselaar, M. E., Cuevas Gozalo, M. C., and Moyano, S.: Avulsion processes at the terminus of low-
721 gradient semi-arid fluvial systems: Lessons from the Río Colorado, Altiplano endorheic basin, Bolivia,
722 *Sedimentary Geology*, 283, 1–14, <https://doi.org/10.1016/j.sedgeo.2012.10.007>, 2013.
- 723 Edmonds, D. A. and Slingerland, R. L.: Mechanics of river mouth bar formation: Implications for the
724 morphodynamics of delta distributary networks, *J. Geophys. Res.*, 112, 2006JF000574,
725 <https://doi.org/10.1029/2006JF000574>, 2007.
- 726 Edmonds, D. A., Paola, C., Hoyal, D. C. J. D., and Sheets, B. A.: Quantitative metrics that describe river
727 deltas and their channel networks, *J. Geophys. Res.*, 116, F04022, <https://doi.org/10.1029/2010JF001955>,
728 2011.
- 729 Edmonds, D. A., Martin, H. K., Valenza, J. M., Henson, R., Weissmann, G. S., Miltenberger, K., Mans,
730 W., Moore, J. R., Slingerland, R. L., Gibling, M. R., Bryk, A. B., and Hajek, E. A.: Rivers in reverse:
731 Upstream-migrating dechannelization and flooding cause avulsions on fluvial fans, *Geology*, 50, 37–41,
732 <https://doi.org/10.1130/G49318.1>, 2022.
- 733 Esri: World Imagery, Esri, Maxar, Relands, CA, 2025.
- 734 Fagherazzi, S.: Self-organization of tidal deltas, *Proc. Natl. Acad. Sci. U.S.A.*, 105, 18692–18695,
735 <https://doi.org/10.1073/pnas.0806668105>, 2008.
- 736 Fagherazzi, S., Edmonds, D. A., Nardin, W., Leonardi, N., Canestrelli, A., Falcini, F., Jerolmack, D. J.,
737 Mariotti, G., Rowland, J. C., and Slingerland, R. L.: Dynamics of river mouth deposits, *Reviews of*
738 *Geophysics*, 53, 642–672, <https://doi.org/10.1002/2014RG000451>, 2015.
- 739 Farley, K. A., Williford, K. H., Stack, K. M., Bhartia, R., Chen, A., De La Torre, M., Hand, K., Goreva,
740 Y., Herd, C. D. K., Hueso, R., Liu, Y., Maki, J. N., Martinez, G., Moeller, R. C., Nelessen, A., Newman,
741 C. E., Nunes, D., Ponce, A., Spanovich, N., Willis, P. A., Beegle, L. W., Bell, J. F., Brown, A. J.,

- 742 Hamran, S.-E., Hurowitz, J. A., Maurice, S., Paige, D. A., Rodriguez-Manfredi, J. A., Schulte, M., and
743 Wiens, R. C.: Mars 2020 Mission Overview, *Space Sci Rev*, 216, 142, [https://doi.org/10.1007/s11214-](https://doi.org/10.1007/s11214-020-00762-y)
744 020-00762-y, 2020.
- 745 Federici, B. and Paola, C.: Dynamics of channel bifurcations in noncohesive sediments, *Water Resources*
746 *Research*, 39, 2002WR001434, <https://doi.org/10.1029/2002WR001434>, 2003.
- 747 Fielding, C. R., Ashworth, P. J., Best, J. L., Prokocki, E. W., and Smith, G. H. S.: Tributary, distributary
748 and other fluvial patterns: What really represents the norm in the continental rock record?, *Sedimentary*
749 *Geology*, 261–262, 15–32, <https://doi.org/10.1016/j.sedgeo.2012.03.004>, 2012.
- 750 Fontana, A., Mozzi, P., and Marchetti, M.: Alluvial fans and megafans along the southern side of the
751 Alps, *Sedimentary Geology*, 301, 150–171, <https://doi.org/10.1016/j.sedgeo.2013.09.003>, 2014.
- 752 Friend, P. F.: *DISTINCTIVE FEATURES OF SOME ANCIENT RIVER SYSTEMS*, 1978.
- 753 Galloway, E.: Process Framework for Describing the Morphologic and Stratigraphic Evolution of Deltaic
754 Depositional Systems, *Deltas: Models for Exploration*, 1975, 87–98, 1975.
- 755 Ganti, V., Chu, Z., Lamb, M. P., Nittrouer, J. A., and Parker, G.: Testing morphodynamic controls on the
756 location and frequency of river avulsions on fans versus deltas: Huanghe (Yellow River), China,
757 *Geophysical Research Letters*, 41, 7882–7890, <https://doi.org/10.1002/2014GL061918>, 2014.
- 758 Gearon, J. H., Martin, H. K., DeLisle, C., Barefoot, E. A., Mohrig, D., Paola, C., and Edmonds, D. A.:
759 Rules of river avulsion change downstream, *Nature*, 634, 91–95, [https://doi.org/10.1038/s41586-024-](https://doi.org/10.1038/s41586-024-07964-2)
760 07964-2, 2024.
- 761 Geleynse, N., Storms, J. E. A., Walstra, D.-J. R., Jagers, H. R. A., Wang, Z. B., and Stive, M. J. F.:
762 Controls on river delta formation; insights from numerical modelling, *Earth and Planetary Science*
763 *Letters*, 302, 217–226, <https://doi.org/10.1016/j.epsl.2010.12.013>, 2011.
- 764 Giosan, L., Syvitski, J., Constantinescu, S., and Day, J.: Climate change: Protect the world’s deltas,
765 *Nature*, 516, 31–33, <https://doi.org/10.1038/516031a>, 2014.
- 766 Hansford, M. R. and Plink-Björklund, P.: River discharge variability as the link between climate and
767 fluvial fan formation, *Geology*, 48, 952–956, <https://doi.org/10.1130/G47471.1>, 2020.
- 768 Hariharan, J., Piliouras, A., Schwenk, J., and Passalacqua, P.: Width-Based Discharge Partitioning in
769 Distributary Networks: How Right We Are, *Geophysical Research Letters*, 49, e2022GL097897,
770 <https://doi.org/10.1029/2022GL097897>, 2022.
- 771 Harris, C. R., Millman, K. J., van der Walt, S. J., Gommers, R., Virtanen, P., Cournapeau, D., Wieser, E.,
772 Taylor, J., Berg, S., Smith, N. J., Kern, R., Picus, M., Hoyer, S., van Kerkwijk, M. H., Brett, M., Haldane,
773 A., del Río, J. F., Wiebe, M., Peterson, P., Gérard-Marchant, P., Sheppard, K., Reddy, T., Weckesser, W.,
774 Abbasi, H., Gohlke, C., and Oliphant, T. E.: Array programming with NumPy, *Nature*, 585, 357–362,
775 <https://doi.org/10.1038/s41586-020-2649-2>, 2020.
- 776 Hartley, A. J., Weissmann, G. S., Nichols, G. J., and Warwick, G. L.: Large Distributive Fluvial Systems:
777 Characteristics, Distribution, and Controls on Development, *Journal of Sedimentary Research*, 80, 167–
778 183, <https://doi.org/10.2110/jsr.2010.016>, 2010.

779 Horton, B. K. and Decelles, P. G.: Modern and ancient Fluvial megafans in the foreland basin system of
780 the central Andes, southern Bolivia: implications for drainage network evolution in fold-thrust belts,
781 2001.

782 Hunter, J. D.: MATPLOTLIB - 2D GRAPHICS ENVIRONMENT, Computing in Science &
783 Engineering, 2007.

784 Isikdogan, F., Bovik, A., and Passalacqua, P.: RivaMap: An automated river analysis and mapping
785 engine, Remote Sensing of Environment, 202, 88–97, <https://doi.org/10.1016/j.rse.2017.03.044>, 2017.

786 Jerolmack, D. J.: Conceptual framework for assessing the response of delta channel networks to Holocene
787 sea level rise, Quaternary Science Reviews, 28, 1786–1800,
788 <https://doi.org/10.1016/j.quascirev.2009.02.015>, 2009.

789 Jerolmack, D. J. and Swenson, J. B.: Scaling relationships and evolution of distributary networks on
790 wave-influenced deltas, Geophysical Research Letters, 34, 2007GL031823,
791 <https://doi.org/10.1029/2007GL031823>, 2007.

792 Jones, L. S. and Schumm, S. A.: Causes of Avulsion: An Overview, in: Fluvial Sedimentology VI, edited
793 by: Smith, N. D. and Rogers, J., Wiley, 169–178, <https://doi.org/10.1002/9781444304213.ch13>, 1999.

794 Ke, W., Shaw, J. B., Mahon, R. C., and Cathcart, C. A.: Distributary Channel Networks as Moving
795 Boundaries: Causes and Morphodynamic Effects, JGR Earth Surface, 124, 1878–1898,
796 <https://doi.org/10.1029/2019JF005084>, 2019.

797 Kelly, S. B. and Olsen, H.: Terminal fans a review with reference to Devonian examples, Sedimentary
798 Geology, 1993.

799 Lauzon, R., Piliouras, A., and Rowland, J. C.: Ice and Permafrost Effects on Delta Morphology and
800 Channel Dynamics, Geophysical Research Letters, 46, 6574–6582,
801 <https://doi.org/10.1029/2019GL082792>, 2019.

802 Leier, A. L., DeCelles, P. G., and Pelletier, J. D.: Mountains, monsoons, and megafans, Geol, 33, 289,
803 <https://doi.org/10.1130/G21228.1>, 2005.

804 Leonardi, N., Canestrelli, A., Sun, T., and Fagherazzi, S.: Effect of tides on mouth bar morphology and
805 hydrodynamics, Journal of Geophysical Research: Oceans, 118, 4169–4183,
806 <https://doi.org/10.1002/jgrc.20302>, 2013.

807 Limaye, A. B., Adler, J. B., Moodie, A. J., Whipple, K. X., and Howard, A. D.: Effect of Standing Water
808 on Formation of Fan-Shaped Sedimentary Deposits at Hypanis Valles, Mars, Geophysical Research
809 Letters, 50, e2022GL102367, <https://doi.org/10.1029/2022GL102367>, 2023.

810 Mahon, R., Hughes, C., Chen, H., and Shaw, J.: Ancient Channel-Mouth Bifurcation Angles on Earth and
811 Mars, The Sedimentary Record, 22, <https://doi.org/10.2110/001c.124824>, 2024.

812 Malin, M. C. and Edgett, K. S.: Evidence for Persistent Flow and Aqueous Sedimentation on Early Mars,
813 2015.

814 Martin, H. K. and Edmonds, D. A.: Avulsion dynamics determine fluvial fan morphology in a cellular
815 model, Geology, 51, 796–800, <https://doi.org/10.1130/G51138.1>, 2023.

- 816 Mendenhall, W., Beaver, R. J., and Beaver, B. M.: Introduction to Probability and Statistics, Brooks/Cole,
817 2012.
- 818 Mohrig, D., Heller, P. L., Paola, C., and Lyons, W. J.: Interpreting avulsion process from ancient alluvial
819 sequences: Guadalope-Matarranya system (northern Spain) and Wasatch Formation (western Colorado),
820 Geological Society of America Bulletin, 2000.
- 821 Morais, E. S. and Montanher, O. C.: Avulsion in a meandering river: floodplain conditions for occurrence
822 and effects in the parent channel, CATENA, 214, 106236, <https://doi.org/10.1016/j.catena.2022.106236>,
823 2022.
- 824 Morón, S., Amos, K., Edmonds, D. A., Payenberg, T., Sun, X., and Thyer, M.: Avulsion triggering by El
825 Niño–Southern Oscillation and tectonic forcing: The case of the tropical Magdalena River, Colombia,
826 GSA Bulletin, 129, 1300–1313, <https://doi.org/10.1130/B31580.1>, 2017.
- 827 Moscariello, A.: Alluvial fans and fluvial fans at the margins of continental sedimentary basins:
828 geomorphic and sedimentological distinction for geo-energy exploration and development, SP, 440, 215–
829 243, <https://doi.org/10.1144/SP440.11>, 2018.
- 830 Nichols, G. J.: STRUCTURAL CONTROLS ON FLUVIAL DISTRIBUTARY SYSTEMS-THE LUNA
831 SYSTEM, NORTHERN SPAIN, 1987.
- 832 Nichols, G. J. and Fisher, J. A.: Processes, facies and architecture of fluvial distributary system deposits,
833 Sedimentary Geology, 195, 75–90, <https://doi.org/10.1016/j.sedgeo.2006.07.004>, 2007.
- 834 Nienhuis, J. H., Ashton, A. D., and Giosan, L.: What makes a delta wave-dominated?, Geology, 43, 511–
835 514, <https://doi.org/10.1130/G36518.1>, 2015.
- 836 Nienhuis, J. H., Hoitink, A. J. F. T., and Törnqvist, T. E.: Future Change to Tide-Influenced Deltas,
837 Geophysical Research Letters, 45, 3499–3507, <https://doi.org/10.1029/2018GL077638>, 2018.
- 838 Nienhuis, J. H., Ashton, A. D., Edmonds, D. A., Hoitink, A. J. F., Kettner, A. J., Rowland, J. C., and
839 Törnqvist, T. E.: Global-scale human impact on delta morphology has led to net land area gain, Nature,
840 577, 514–518, <https://doi.org/10.1038/s41586-019-1905-9>, 2020.
- 841 North, C. P. and Warwick, G. L.: Fluvial Fans: Myths, Misconceptions, and the End of the Terminal-Fan
842 Model, Journal of Sedimentary Research, 77, 693–701, <https://doi.org/10.2110/jsr.2007.072>, 2007.
- 843 Olariu, C. and Bhattacharya, J. P.: Terminal distributary channels and delta front architecture of river-
844 dominated delta systems, Journal of Sedimentary Research, 76, 212–233,
845 <https://doi.org/10.2110/jsr.2006.026>, 2006.
- 846 Ori, G. G., Marinangeli, L., and Baliva, A.: Terraces and Gilbert-type deltas in crater lakes in Ismenius
847 Lacus and Memnonia (Mars), J. Geophys. Res., 105, 17629–17641,
848 <https://doi.org/10.1029/1999JE001219>, 2000.
- 849 Owen, A., Nichols, G. J., Hartley, A. J., Weissmann, G. S., and Scuderi, L. A.: Quantification of a
850 Distributive Fluvial System: The Salt Wash DFS of the Morrison Formation, SW U.S.A., Journal of
851 Sedimentary Research, 85, 544–561, <https://doi.org/10.2110/jsr.2015.35>, 2015.

- 852 Paniagua-Arroyave, J. F. and Nienhuis, J. H.: The Quantified Galloway Ternary Diagram of Delta
853 Morphology, *JGR Earth Surface*, 129, e2024JF007878, <https://doi.org/10.1029/2024JF007878>, 2024.
- 854 Paola, C., Twilley, R. R., Edmonds, D. A., Kim, W., Mohrig, D., Parker, G., Viparelli, E., and Voller, V.
855 R.: Natural Processes in Delta Restoration: Application to the Mississippi Delta, *Annu. Rev. Mar. Sci.*, 3,
856 67–91, <https://doi.org/10.1146/annurev-marine-120709-142856>, 2011.
- 857 Parker, G., Paola, C., Whipple, K. X., and Mohrig, D.: ALLUVIAL FANS FORMED BY
858 CHANNELIZED FLUVIAL AND SHEET FLOW. I: THEORY, *Journal OF Hydraulic Engineering*,
859 985–995, 1998.
- 860 Passalacqua, P.: The Delta Connectome: A network-based framework for studying connectivity in river
861 deltas, *Geomorphology*, 277, 50–62, <https://doi.org/10.1016/j.geomorph.2016.04.001>, 2017.
- 862 Pearson, S. G., Van Prooijen, B. C., Elias, E. P. L., Vitousek, S., and Wang, Z. B.: Sediment
863 Connectivity: A Framework for Analyzing Coastal Sediment Transport Pathways, *JGR Earth Surface*,
864 125, e2020JF005595, <https://doi.org/10.1029/2020JF005595>, 2020.
- 865 Piliouras, A., Lauzon, R., and Rowland, J. C.: Unraveling the Combined Effects of Ice and Permafrost on
866 Arctic Delta Morphodynamics, *JGR Earth Surface*, 126, e2020JF005706,
867 <https://doi.org/10.1029/2020JF005706>, 2021.
- 868 Pizzuto, J. E.: Sediment diffusion during overbank flows, *Sedimentology*, 34, 301–317,
869 <https://doi.org/10.1111/j.1365-3091.1987.tb00779.x>, 1987.
- 870 Plink-Björklund, P.: Distributive Fluvial Systems: Fluvial and Alluvial Fans, in: *Encyclopedia of*
871 *Geology*, Elsevier, 745–758, <https://doi.org/10.1016/B978-0-08-102908-4.00015-1>, 2021.
- 872 Radebaugh, J., Ventra, D., Lorenz, R. D., Farr, T., Kirk, R., Hayes, A., Malaska, M. J., Birch, S., Liu, Z.
873 Y.-C., Lunine, J., Barnes, J., Le Gall, A., Lopes, R., Stofan, E., Wall, S., and Paillou, P.: Alluvial and
874 fluvial fans on Saturn’s moon Titan reveal processes, materials and regional geology, *SP*, 440, 281–305,
875 <https://doi.org/10.1144/SP440.6>, 2018.
- 876 Rahman, M. M., Howell, J. A., and MacDonald, D. I. M.: Quantitative analysis of crevasse-splay systems
877 from modern fluvial settings, *Journal of Sedimentary Research*, 92, 751–774,
878 <https://doi.org/10.2110/jsr.2020.067>, 2022.
- 879 Reitz, M. D. and Jerolmack, D. J.: Experimental alluvial fan evolution: Channel dynamics, slope controls,
880 and shoreline growth, *J. Geophys. Res.*, 117, 2011JF002261, <https://doi.org/10.1029/2011JF002261>,
881 2012.
- 882 Saito, Y., Thanawat, J., Chaimanee, N., Jarupongsakul, T., and Syvitski, J. P. M.: Shrinking Megadeltas
883 in Asia: Sea-level Rise and Sediment Reduction Impacts from Case Study of the Chao Phraya Delta The
884 Holocene Red River Delta, Vietnam View project Global Risks and research priorities for coastal
885 subsidence View project Shrinking Megadeltas in Asia: Sea-level Rise and Sediment Reduction Impacts
886 from Case Study of the Chao Phraya Delta, 2007.
- 887 Schumm, S. A.: *The fluvial system*, Food and Agriculture Organization of the United Nations, 1977.
- 888 Schwanghart, W. and Kuhn, N. J.: TopoToolbox: A set of Matlab functions for topographic analysis,
889 *Environmental Modelling & Software*, 25, 770–781, <https://doi.org/10.1016/j.envsoft.2009.12.002>, 2010.

- 890 Seybold, H., Andrade, J. S., and Herrmann, H. J.: Modeling river delta formation, *Proc. Natl. Acad. Sci.*
891 *U.S.A.*, 104, 16804–16809, <https://doi.org/10.1073/pnas.0705265104>, 2007.
- 892 Seybold, H., Rothman, D. H., and Kirchner, J. W.: Climate’s watermark in the geometry of stream
893 networks, *Geophysical Research Letters*, 44, 2272–2280, <https://doi.org/10.1002/2016GL072089>, 2017.
- 894 Seybold, H. J., Kite, E., and Kirchner, J. W.: Branching geometry of valley networks on Mars and Earth
895 and its implications for early Martian climate, *Sci. Adv.*, 4, eaar6692,
896 <https://doi.org/10.1126/sciadv.aar6692>, 2018.
- 897 Shaw, J. B., Miller, K., and McElroy, B.: Island Formation Resulting From Radially Symmetric Flow
898 Expansion, *JGR Earth Surface*, 123, 363–383, <https://doi.org/10.1002/2017JF004464>, 2018.
- 899 Singh, H., Parkash, B., and Gohain, K.: Facies analysis of the Kosi megafan deposits, *Sedimentary*
900 *Geology*, 85, 87–113, [https://doi.org/10.1016/0037-0738\(93\)90077-I](https://doi.org/10.1016/0037-0738(93)90077-I), 1993.
- 901 Sinha, R.: The Great avulsion of Kosi on 18 August 2008, *Current Science*, 97, 429–433, 2009.
- 902 Slingerland, R. and Smith, N. D.: Necessary conditions for a meandering-river avulsion, *Geol*, 26, 435,
903 [https://doi.org/10.1130/0091-7613\(1998\)026%253C0435:NCFAMR%253E2.3.CO;2](https://doi.org/10.1130/0091-7613(1998)026%253C0435:NCFAMR%253E2.3.CO;2), 1998.
- 904 Slingerland, R. and Smith, N. D.: RIVER AVULSIONS AND THEIR DEPOSITS, *Annu. Rev. Earth*
905 *Planet. Sci.*, 32, 257–285, <https://doi.org/10.1146/annurev.earth.32.101802.120201>, 2004.
- 906 Smart, J. S.: QUANTITATIVE PROPERTIES OF DELTA CHANNEL NETWORKS, 1971.
- 907 Syvitski, J. P. M. and Brakenridge, G. R.: Causation and avoidance of catastrophic flooding along the
908 Indus River, Pakistan, *GSAT*, 23, 4–10, <https://doi.org/10.1130/GSATG165A.1>, 2013.
- 909 Syvitski, J. P. M., Kettner, A. J., Overeem, I., Hutton, E. W. H., Hannon, M. T., Brakenridge, G. R., Day,
910 J., Vörösmarty, C., Saito, Y., Giosan, L., and Nicholls, R. J.: Sinking deltas due to human activities,
911 *Nature Geosci*, 2, 681–686, <https://doi.org/10.1038/ngeo629>, 2009.
- 912 Tebolt, M. and Goudge, T. A.: Global investigation of martian sedimentary fan features: Using
913 stratigraphic analysis to study depositional environment, *Icarus*, 372, 114718,
914 <https://doi.org/10.1016/j.icarus.2021.114718>, 2022.
- 915 Tejedor, A., Longjas, A., Zaliapin, I., and Fofoula-Georgiou, E.: Delta channel networks: 1. A graph-
916 theoretic approach for studying connectivity and steady state transport on deltaic surfaces, *Water*
917 *Resources Research*, 51, 3998–4018, <https://doi.org/10.1002/2014WR016577>, 2015.
- 918 Tejedor, A., Longjas, A., Edmonds, D. A., Zaliapin, I., Georgiou, T. T., Rinaldo, A., and Fofoula-
919 Georgiou, E.: Entropy and optimality in river deltas, *Proc. Natl. Acad. Sci. U.S.A.*, 114, 11651–11656,
920 <https://doi.org/10.1073/pnas.1708404114>, 2017.
- 921 Törnqvist, T. E. and Bridge, J. S.: Spatial variation of overbank aggradation rate and its influence on
922 avulsion frequency, *Sedimentology*, 49, 891–905, <https://doi.org/10.1046/j.1365-3091.2002.00478.x>,
923 2002.

- 924 Trampush, S. M. and Hajek, E. A.: Preserving proxy records in dynamic landscapes: Modeling and
925 examples from the Paleocene-Eocene Thermal Maximum, *Geology*, 45, 967–970,
926 <https://doi.org/10.1130/G39367.1>, 2017.
- 927 Trauth, M. H.: *MATLAB® Recipes for Earth Sciences*, 2006.
- 928 Ventra, D. and Clarke, L. E.: Geology and geomorphology of alluvial and fluvial fans: current progress
929 and research perspectives, *SP*, 440, 1–21, <https://doi.org/10.1144/SP440.16>, 2018.
- 930 Virtanen, P., Gommers, R., Oliphant, T. E., Haberland, M., Reddy, T., Cournapeau, D., Burovski, E.,
931 Peterson, P., Weckesser, W., Bright, J., van der Walt, S. J., Brett, M., Wilson, J., Millman, K. J.,
932 Mayorov, N., Nelson, A. R. J., Jones, E., Kern, R., Larson, E., Carey, C. J., Polat, İ., Feng, Y., Moore, E.
933 W., VanderPlas, J., Laxalde, D., Perktold, J., Cimrman, R., Henriksen, I., Quintero, E. A., Harris, C. R.,
934 Archibald, A. M., Ribeiro, A. H., Pedregosa, F., van Mulbregt, P., Vijaykumar, A., Bardelli, A. P.,
935 Rothberg, A., Hilboll, A., Kloeckner, A., Scopatz, A., Lee, A., Rokem, A., Woods, C. N., Fulton, C.,
936 Masson, C., Häggström, C., Fitzgerald, C., Nicholson, D. A., Hagen, D. R., Pasechnik, D. V., Olivetti, E.,
937 Martin, E., Wieser, E., Silva, F., Lenders, F., Wilhelm, F., Young, G., Price, G. A., Ingold, G. L., Allen,
938 G. E., Lee, G. R., Audren, H., Probst, I., Dietrich, J. P., Silterra, J., Webber, J. T., Slavič, J., Nothman, J.,
939 Buchner, J., Kulick, J., Schönberger, J. L., de Miranda Cardoso, J. V., Reimer, J., Harrington, J.,
940 Rodríguez, J. L. C., Nunez-Iglesias, J., Kuczynski, J., Tritz, K., Thoma, M., Newville, M., Kümmerer,
941 M., Bolingbroke, M., Tartre, M., Pak, M., Smith, N. J., Nowaczyk, N., Shebanov, N., Pavlyk, O.,
942 Brodtkorb, P. A., Lee, P., McGibbon, R. T., Feldbauer, R., Lewis, S., Tygier, S., Sievert, S., Vigna, S.,
943 Peterson, S., More, S., Pudlik, T., et al.: SciPy 1.0: fundamental algorithms for scientific computing in
944 Python, *Nature Methods*, 17, 261–272, <https://doi.org/10.1038/s41592-019-0686-2>, 2020.
- 945 Vulis, L., Tejedor, A., Ma, H., Nienhuis, J. H., Broaddus, C. M., Brown, J., Edmonds, D. A., Rowland, J.
946 C., and Foufoula-Georgiou, E.: River Delta Morphotypes Emerge From Multiscale Characterization of
947 Shorelines, *Geophysical Research Letters*, 50, e2022GL102684, <https://doi.org/10.1029/2022GL102684>,
948 2023.
- 949 Walker, H. J.: Arctic Deltas, *Journal of Coastal Research*, 14, 718–738, 1998.
- 950 Wall, S., Hayes, A., Bristow, C., Lorenz, R., Stofan, E., Lunine, J., Le Gall, A., Janssen, M., Lopes, R.,
951 Wye, L., Soderblom, L., Paillou, P., Aharonson, O., Zebker, H., Farr, T., Mitri, G., Kirk, R., Mitchell, K.,
952 Notarnicola, C., Casarano, D., and Ventura, B.: Active shoreline of Ontario Lacus, Titan: A
953 morphological study of the lake and its surroundings, *Geophysical Research Letters*, 37, 2009GL041821,
954 <https://doi.org/10.1029/2009GL041821>, 2010.
- 955 Wang, J. and Plink-Björklund, P.: Stratigraphic complexity in fluvial fans: Lower Eocene Green River
956 Formation, Uinta Basin, USA, *Basin Research*, 31, 892–919, <https://doi.org/10.1111/bre.12350>, 2019.
- 957 Waskom, M.: seaborn: statistical data visualization, *Journal of Open Source Software*, 6, 3021,
958 <https://doi.org/10.21105/joss.03021>, 2021.
- 959 Weissman, G. S., Hartley, A. J., Nichols, G. J., Scuderi, L. A., Olson, M., Buehler, H., and Banteah, R.:
960 Fluvial form in modern continental sedimentary basins: Distributive fluvial systems,
961 <https://doi.org/10.1016/j.geo>, 2010.
- 962 Weissmann, G. S., Hartley, A. J., Nichols, G. J., Scuderi, L. A., Olson, M., Buehler, H., and Banteah, R.:
963 Fluvial form in modern continental sedimentary basins: Distributive fluvial systems, *Geology*, 38, 39–42,
964 <https://doi.org/10.1130/G30242.1>, 2010.

- 965 Weissmann, G. S., Hartley, A. J., Scuderi, L. A., Nichols, G. J., Owen, A., Wright, S., Felicia, A. L.,
966 Holland, F., and Anaya, F. M. L.: Fluvial geomorphic elements in modern sedimentary basins and their
967 potential preservation in the rock record: A review, *Geomorphology*, 250, 187–219,
968 <https://doi.org/10.1016/j.geomorph.2015.09.005>, 2015.
- 969 Witek, P. P. and Czechowski, L.: Dynamical modelling of river deltas on Titan and Earth, *Planetary and*
970 *Space Science*, 105, 65–79, <https://doi.org/10.1016/j.pss.2014.11.005>, 2015.
- 971 Wolinsky, M. A., Edmonds, D. A., Martin, J., and Paola, C.: Delta allometry: Growth laws for river
972 deltas, *Geophysical Research Letters*, 37, 2010GL044592, <https://doi.org/10.1029/2010GL044592>, 2010.
- 973 Wood, L. J.: Quantitative geomorphology of the Mars Eberswalde delta, *Geological Society of America*
974 *Bulletin*, 118, 557–566, <https://doi.org/10.1130/B25822.1>, 2006.
- 975 Wright, L. D.: Sediment transport and deposition at river mouths: A synthesis, *Geol Soc America Bull*,
976 88, 857, [https://doi.org/10.1130/0016-7606\(1977\)88%253C857:STADAR%253E2.0.CO;2](https://doi.org/10.1130/0016-7606(1977)88%253C857:STADAR%253E2.0.CO;2), 1977.
- 977 Xu, Z. and Plink-Björklund, P.: Quantifying Formative Processes in River- and Tide-Dominated Deltas
978 for Accurate Prediction of Future Change, *Geophysical Research Letters*, 50, e2023GL104434,
979 <https://doi.org/10.1029/2023GL104434>, 2023.
- 980 Yang, H.: Numerical investigation of avulsions in gravel-bed braided rivers, *Hydrological Processes*, 34,
981 3702–3717, <https://doi.org/10.1002/hyp.13837>, 2020.
- 982